ASSESSING METEOROLOGICAL AND VEGETATION DROUGHT INDICES AGAINST SOIL MOISTURE MEASUREMENTS OVER TWENTE REGION, THE NETHERLANDS

PATIENCE KATHEO MUSILA
July 2020

SUPERVISORS:
Dr. Ir. R. van der Velde
Dr. Ir. S. Salama

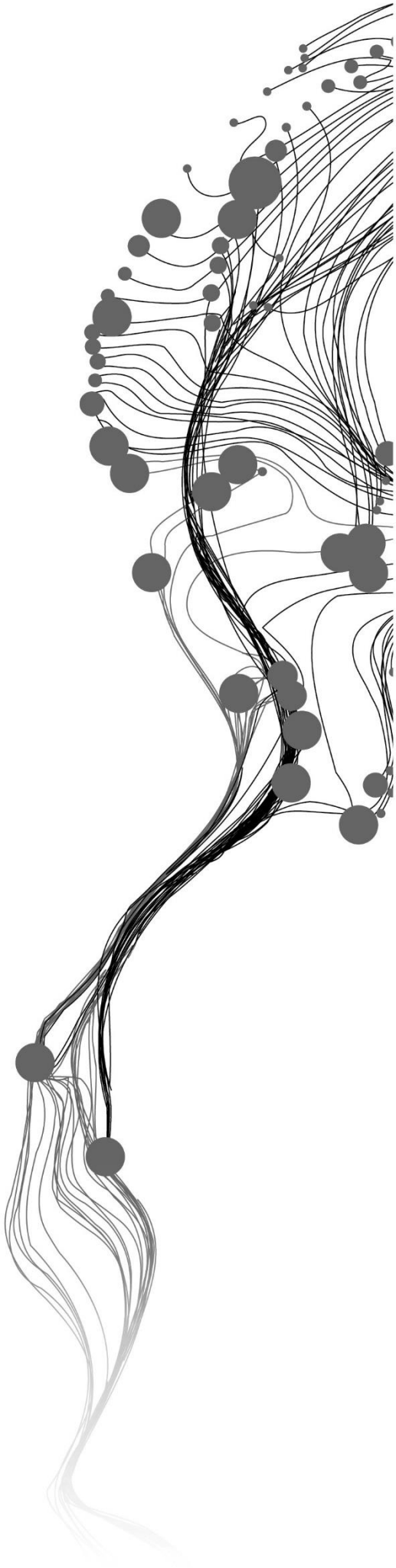

ASSESSING METEOROLOGICAL AND VEGETATION DROUGHT INDICES AGAINST SOIL MOISTURE MEASUREMENTS OVER TWENTE REGION, THE NETHERLANDS

PATIENCE KATHEO MUSILA
Enschede, The Netherlands, July 2021

Thesis submitted to the Faculty of Geo-Information Science and Earth Observation of the University of Twente in partial fulfilment of the requirements for the degree of Master of Science in Geo-information Science and Earth Observation.
Specialization: Water Resources Management

SUPERVISORS:
Dr. Ir. R. van der Velde
Dr. Ir. S. Salama

THESIS ASSESSMENT BOARD:
Prof. Dr. Z. Bob Su (Chair)
Dr. Ir. D.C.M. Augustijn (External Examiner, University of Twente)

ABSTRACT

Drought events of high precipitation deficits have become rampant in the Netherlands in the recent years. The year 2018 was recorded as the worst drought with associated huge impacts on the economy, agriculture, and navigation industry. Drought indices (often unitless, and between 1 and -1) have provided a reliable way of quantifying the characteristics of droughts by comparing prevailing climatic conditions to their long term normal (mean). This research investigated the potential of meteorological drought indices (the Standardized Precipitation Index, SPI, and the Standardized Precipitation Evapotranspiration Index, SPEI) in combination with vegetation drought indices (the Normalized Difference Vegetation Index Anomaly, NDVI-A and the Normalized Difference Water Index Anomaly, NDWI-A) to quantify agricultural droughts as observed by anomalies of in-situ soil profile measurements in the Twente region, The Netherlands. These indices provided flexibility in detecting short term dry events that occur in meteorological and agricultural droughts at two given timescales (16-day and monthly). For meteorological indices, higher correlations of SPEI over SPI in relation to soil moisture anomalies, indicated the importance of incorporating the water demand component that corresponds to the role of soil moisture (provision of water vapor) which is not accounted for by SPI. For the vegetation drought indices, high correlations of NDWI-A over NDVI-A in relation to soil moisture anomalies, provided insight on the complex relationship between various leaf components (leaf water content and chlorophyll content ("greenness") and soil moisture. When soil moisture anomalies were lagged backwards in months, SPEI yielded a higher correlation over SPI with a lag of one month. This illustrated that impacts of the water balance anomalies (high precipitation deficit, high temperatures, and increased radiation) are best observed in soil moisture after one month. The NDVI-A correlation illustrated a slight increase with a lag of one month indicating that observed vegetation "greenness" responds optimally to antecedent soil moisture conditions of one month. Conversely, the NDWI-A reduced its correlation with one-month lag but had a high correlation at zero-time lag. This illustrated that the leaf water content responds quicker to ongoing soil moisture variations without delay than observed "greenness". The research concluded that SPEI and NDWI-A were the preferred drought indices for estimating agricultural droughts based on their high and quick response to soil moisture anomalies in Twente region.

Key words meteorological drought indices. vegetation drought indices. SPI. SPEI. NDWI-A. NDVI-A. soil moisture. surface soil moisture anomalies. root zone soil moisture anomalies.

ACKNOWLEDGEMENTS

Special thanks to the Dutch Government for giving me the opportunity and support to advance my skills and knowledge in the field of Remote sensing at the prestigious Faculty of Geo-information Science and Earth Observation, in Netherlands. I thank all the staff at the Department of Water Resources Management for providing a conducive space for learning the complexities of water as a limited natural resource and how to monitor it in space.

My sincere gratitude goes to my supervisors, Dr. Ir. R. van der Velde and Dr. Ir. S. Salama for the determined support in ensuring successful completion of my research. I have gained skills in quantitative data analysis and interpretation of results useful for future endeavours. I would also like to thank my Department mentor Ir. A.M. van Lieshout for his support on student wellbeing especially during the Covid-19 period.

I am grateful to God for keeping my family and I safe and of good health throughout my study period. Lastly, I am grateful for my colleagues and friends who became family in our two -year study in Enschede, The Netherlands.

Patience Katheo Musila

TABLE OF CONTENTS

LIST OF FIGURES

LIST OF TABLES

LIST OF ABBREVIATIONS

AVHHRR	Advanced Very-High-Resolution Radiometer
CDF	Cumulative Distribution Function
ETref	Crop Reference Evapotranspiration
MODIS	MODerate resolution Imaging Spectro-radiometer
NDVI	Normalized Difference Vegetation Index
NDVIA	Normalized Difference Vegetation Index Anomaly
NDWI	Normalized Difference Water Index
NDWIA	Normalized Difference Water Index Anomaly
NIR	Near Infrared
PDF	Probability Distribution Function
PDSI	Palmer Drought Severity Index
R	Correlation Coefficient
RZSM	Root zone soil moisture
RZSMA	Root zone soil moisture Anomaly
SMAP	Soil Moisture Active Passive
SSM	Surface Soil Moisture
SPI	Standardized Precipitation Index
SPEI	Standardized Precipitation Evapotranspiration Index

1. INTRODUCTION

1.1. Scientific Background

Low precipitation amounts, usually accompanied by warm surface temperatures trigger a reduction in moisture levels, often referred to as drought (Mishra & Singh, 2010; Sivakumar et al., 2010). Other climatic factors such as high winds, low relative humidity exacerbate the occurrence of the event (Sivakumar et al., 2010). Drought is perceived to occur gradually, probably for several months and years. However, the onset of drought can also be rapid in instances where extreme atmospheric anomalies persist only for several weeks within a region, referred to as 'flash droughts' (Osman et al., 2021; Svoboda et al., 2002). Such flash droughts have been reported to have detrimental effects to the environment and society due to insufficient early warnings (Osman et al., 2021; Zhang & Yuan, 2020).

There are expected changes in the frequency and severity of droughts in the 21st century in Europe as articulated by climate change reports (Dai, 2013; McCarthy et al., 2001; Pachauri & Meyer, 2014). Major drought events that have been recorded in many parts of Europe, including Northern and Western Europe, for the last thirty years occurred in 1976, 1989, 1991, 2003 and recently, in 2018 during the summers accompanied by heat waves (Feyen & Dankers, 2009; Fu et al., 2020). Spatio-temporal analysis of droughts in Europe pointed out that past droughts over 250 years ago had characteristics of longer duration, higher intensity and larger spatial extent than the drought events seen in the recent years (Brázdil et al., 2018).

The high spatial and temporal variability of drought events and associated impacts makes it challenging to monitor drought onset and termination as well as its magnitude /severity (Brown et al., 2008). The effects of drought in an area are cumulative in nature and can be observed during and after termination of the drought event (Sivakumar et al., 2010). In an attempt to define drought characteristics, Byun & Wilhite, (1999) defined the severity of drought as the consecutive dry periods below a certain threshold of climatic anomalies. The severity can also involve the impacts observed on water resources, such as depletion in soil moisture and water reservoir levels.

A drought indicator is defined as a variable of which a change in its behavior gives information on the potential of drought-related stress (Yihdego et al., 2019). Drought indicators commonly used in drought studies include rainfall, temperature, soil moisture, stream flow to monitor various types of drought. These drought indicators are singly or in combination converted to standardized drought indices (unitless numerical value and between 1 and -1) (Zargar et al., 2011). A drought index is a measure of the deviation

of drought indicators from the normal moisture conditions (Van Loon, 2015). Drought indices have been developed to quantify drought events in terms of severity, duration, intensity and spatial extent (Mishra & Singh, 2010). Mishra & Singh, (2010) outline an overview of numerous drought indices, their strengths, and weaknesses in monitoring drought studies worldwide.

1.1.1. Meteorological drought indices

Meteorological drought caused by accumulation of precipitation deficits, is the key driver of other types of drought (Spinoni et al., 2013; S. Vicente-Serrano et al., 2004). Meteorological drought indices have been developed to monitor this type of drought. The Palmer Drought Severity Index, PDSI (Palmer, 1965), was among the initial meteorological indices developed. The index considers the water balance by incorporating several variables including precipitation, evapotranspiration, and soil water capacity in its computation. However, the soil moisture estimations are complex and parameters used in its computation are only tested for regions in the United States, limiting further application in other regions (Akinremi et al., 1996; S. M. Vicente-Serrano et al., 2011).

Complexities associated with the PDSI formulation led to the development of Standardized Precipitation Index, SPI (Mckee et al., 1993) and Standardized Precipitation Evapotranspiration Index, SPEI (S. M. Vicente-Serrano et al., 2010) that involve simple computations using readily available climatological variables. SPI and SPEI have been widely used due to their ability to quantify climatological anomalies for various periods (referred to as 'timescales') allowing for monitoring of short-term and long-term drought events (S. M. Vicente-Serrano et al., 2011).

The SPI is computed as normalized values of the probability distribution of rainfall recorded in an area (usually > 30 years rainfall) for a certain period and quantifies the precipitation deficits as dry events of different degrees of severity (see Table 1) (Mckee et al., 1993). SPI has garnered wide use on drought intensity / severity assessment (Naresh et al., 2009; Spinoni et al., 2013) and other applications such as estimation of soil moisture (Gwak et al., 2017; Sims et al., 2002).

SPEI was developed to improve existing meteorological drought indices, such as SPI, that only considers precipitation as the driving factor for drought and the simplify the complexities of PDSI. It's similar to SPI in its computation of standardization. However, SPEI is developed from a water balance by introducing the demand factor (reference evapotranspiration) to the supply (precipitation) component (Vicente-Serrano et al., 2006; 2010). The water balance is the difference between precipitation and crop reference evapotranspiration (Vicente-Serrano et al., 2006; 2010). While SPI values are derived from the normalization of precipitation probability distribution, SPEI values are computed from the normalization of the water balance probability distribution (Van Oijen et al., 2014).

Table 1: Standardized Precipitation Index drought severity categories

SPI values	Drought category
SPI ≥ 2.0	Extremely wet
≤ 1.5 SPI < 2.0	Very wet
≤ 1.0 SPI < 1.5	Moderately wet
-1.0 < SPI < 1.0	Near Normal
-1.5 < SPI ≤ -1.0	Moderate dry
-2.0 < SPI ≤ -1.5	Severely dry
SPI ≤ -2.0	Extremely dry

Note. Adapted from "The relationship of drought frequency and duration to time scales" by Mckee, T. B., Doesken, N. J., & Kleist, J. 1993, *Eighth Conference on Applied Climatology*, 17–22. Copyright 1993.

Many studies have successfully used SPI and SPEI in combination to compare temporal variations of droughts and their degree of severity (Mehr & Babak, 2019; Tirivarombo et al., 2018), in estimation of soil moisture (Ariyanto et al., 2020), for quantification of drought impact on crop yield (Peña-Gallardo et al., 2019) among other applications.

1.1.2. Agricultural drought indices

The physiological and biochemical processes in vegetation are highly depended on soil moisture variability (Carter, 1994; Peñuelas et al., 1994). Methods used for monitoring vegetation response to soil moisture variability include the use of crop production yields (Peña-Gallardo et al., 2019; Potop et al., 2009) and tree ring analysis (Abrams et al., 1998). These methods suffer from spatial and temporal limitation due to limited time series data for drought analysis and lack of comparability between drought effects on vegetation across various regions (S. M. Vicente-Serrano, 2007).

Remote sensing methods provide information on the amount of radiation absorbed and reflected by plant leaves (Gallo et al., 1985). Water stressed vegetation show a variation in their spectral signatures (reflected radiation) due to altered leaf components such as the leaf water content, leaf pigments, amount of dry matter and leaf area index (Wang et al., 2008). Commonly used remote-sensed vegetation indices for monitoring vegetation response to drought conditions include The Normalized Difference Vegetation Index (NDVI) and associated vegetation indices (Vegetation Condition Index, VCI, and Enhanced Vegetation Index, EVI). The NDVI is estimated from the near infrared (NIR) and visible red bands due to their sensitivity to plant's chlorophyll content, a measure of "vegetation greenness". An assumption follows that there exists a relationship between the "greenness" observed by satellite sensors and climate variability in a region (Di et al., 1994; Gutman, 1990; Ji & Peters, 2003).

The NDVI solely, is limited in identifying drought and non-drought conditions (Anyamba & Tucker, 2012). Therefore, NDVI anomalies have been developed as standardized values computed from historical NDVI values to quantify temporal variations of the NDVI (Anyamba & Tucker, 2012; Li et al., 2014; Thenkabail et al., 2004; Wgnn & Vmi, 2020). Many studies have investigated the relationship between NDVI anomalies and climatic anomalies to quantify drought occurrences in vegetation (Nanzad et al., 2019; Nicholson & Farrar, 1994; Udelhoven et al., 2009).

Another remote-sensed vegetation index is the Normalized Difference Water Index (NDWI) that provides information on the leaf water content (Gu et al., 2007). This is through the sensitivity of the near infrared (NIR) and shortwave wave infrared (SWIR) bands, to changes in leaf water content (Gao, 1996). Similar to the NDVI, anomalies of NDWI have been developed from historical NDWI estimates to quantitively assess drought on vegetation, where negative anomalies indicate water stressed vegetation (Anderson et al., 2010).

Many studies have used the NDWI anomalies (NDWI-A) and NDVI anomalies (NDVI-A) in combination as proxies for agricultural drought, and compared them with climatological anomalies to reliably monitor such drought occurrences (Anderson et al., 2010; Mladenova et al., 2020; Nanzad et al., 2019; Nicholson & Farrar, 1994; Paruelo & Lauenroth, 1995). In other drought monitoring studies, these vegetation index anomalies have been used to reflect to soil moisture variability (Gu et al., 2008; West et al., 2018)

1.1.3. Soil moisture

Soil moisture generally refers to the water content found in the unsaturated zone of the soil profile and exhibits heterogeneity, among other characteristics, in its distribution both vertically and horizontally in such soil profiles (Seneviratne et al., 2010). Soil moisture has a role in the water and energy cycles whereby it's a source of atmospheric moisture through evaporation from bare soil and transpiration from vegetation (Seneviratne et al., 2010).

The relationship between soil moisture and climatic components, such as precipitation and Evapotranspiration (ET) involves several processes that can be explained in feedback loops (see Figure 1). Relationship C indicates how increase in precipitation leads to increase in soil moisture levels with the assumption that the soils are not saturated prior to precipitation fall. Relationship A indicates high soil moisture levels lead to high evapotranspiration rates and holds more when soil moisture is the limiting factor (Seneviratne et al., 2010). The negative arrow in relationship A indicates the existence of a negative relationship whereby increased ET rates lead to reduced soil moisture levels. Relationship B indicates

uncertainty that exists in that high ET rates lead to high precipitation amounts or lead to reduced soil moisture that reduces atmospheric moisture needed for cloud formation (Seneviratne et al., 2010).

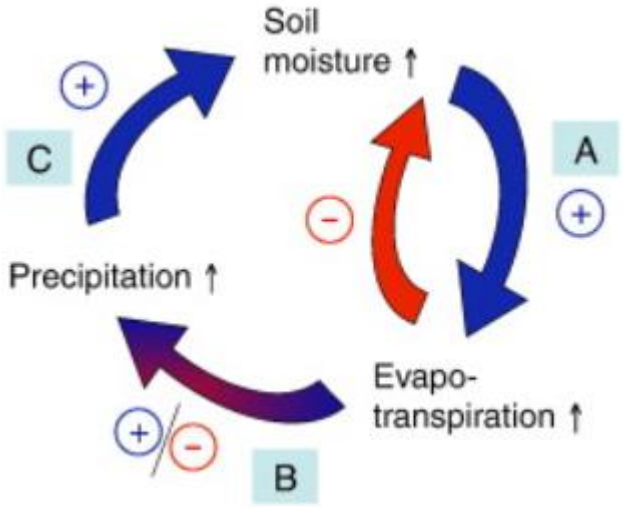

Figure 1: A schematic representation of the of the physical processes that contribute to soil moisture precipitation coupling and feedbacks. Adapted from "Investigating soil moisture-climate interactions in a changing climate" by Seneviratne, S. I., Corti, T., Davin, E. L., Hirschi, M., Jaeger, E. B., Lehner, I., Orlowsky, B., & Teuling, A. J. 2010, A review. In *Earth-Science Reviews* (Vol. 99, Issues 3–4, pp. 125–161). Copyright 2010 by Elsevier.

Based on the above physical processes of soil moisture, the adequate soil moisture levels ensure optimum photosynthetic processes and transpiration rates in vegetation with the availability of incoming shortwave radiation and atmospheric carbon dioxide (CO_2) (Sellers et al., 1997). Vegetation response to changes in soil moisture conditions exists with a time delay observed to be as a result of the ability of the roots to maintain the plant's optimum activities through the uptake of soil moisture until its depleted (Gutman, 1990). Soil moisture has been considered a good drought indicator due to its contribution to vegetation growth (Di et al., 1994) and its relation to recent precipitation depicting drought potential within a region (Keyantash & Dracup, 2002). Moisture in the top layers of the soil profile relates to the short term precipitation and can be seen as a measure of meteorological drought while moisture in the root zone affects different stages of crop growth by ensuring sufficient is water available for transpiration and is a good measure of agricultural drought (Holzman, Rivas & Piccolo, 2014; Keyantash & Dracup, 2002).

1.2. Problem statement

The National meteorological agency in Netherlands, Koninklijk Nederlands Meteorologisch Instituut (KNMI) reported a uniform increase in temperatures across the country from 2018, and increased solar radiation occurring in the inland regions compared to the coastal area (KNMI, 2020). These occurrences come after the earlier climate change scenarios report, labelled KNMI'14, that pointed out The Netherlands and the neighbouring countries have been facing an increase in temperatures over the last 50 years, linked to increased winds in winter months and increased solar radiance in summer months (van

den Hurk et al., 2014). The 2018 drought experienced in the Netherlands motivated various regional drought assessments in the country (Philip et al., 2020; Weijers, 2020).

The potential precipitation deficit (Flach & Phillips, 2018; Sluijter et al., 2018), which is the common drought indicator used for quantifying drought severity across the country, has been recording increasingly high values for the southern and eastern parts of the country especially during the summer period (KNMI, 2020; Philip et al., 2020). The precipitation deficit values are calculated from April 1st to September 30th (summer period) ignoring dry events in the winter season (Weijers, 2020). The high precipitation deficit values recorded have been associated with reduced precipitation amounts, an increase in temperatures and global radiation, that are the key drivers of agricultural drought in the region. (Philip et al., 2020). However, how these precipitation deficits vary at different time scales remains elusive.

The research introduced the use of standardized (with mean of zero and standard deviation of one) drought indices to capture the reported droughts and put them in a historical perspective to determine their frequency and severity. These indices included meteorological drought indices (SPI and SPEI) and vegetation drought indices /anomalies (NDVI-A and NDWI-A). The drought indices had the advantage of analyzing drought in multi-temporal scales making them suitable to capture shot-term meteorological and agricultural droughts that are highly depended on each other through the role of soil moisture in the hydrological cycle.

SPI and SPEI were selected to evaluate how variability in one or more climatic parameters (precipitation variability, radiation, temperatures) influence the occurrence of drought and how soil moisture captures such droughts in Twente. The vegetation anomalies of NDVI and NDWI (NDVI-A and NDWI-A, respectively) provided an opportunity to use remote sensed estimates to monitor vegetation. While the NDVI gives information on the leaf "greenness" associated with chlorophyll content (Rouse et al., 1974), the NDWI gives information on the leaf water content (Gao, 1996). These differences motivated the selection of these vegetation indices to examine their responses to climatic anomalies and soil moisture variations. The standardized nature of all the drought indices allowed for their computation at 16-day and monthly timescales to detect the shortest dry events in the region.

Thus, the meteorological and vegetation drought indices were selected to determine their relationship with observed soil moisture anomalies related to agricultural droughts

1.3. Research objectives

The main objective of research was to assess the potential of meteorological and remote sensing-based drought indices in detecting agricultural drought as observed in profile soil moisture measurements.

The specific objectives addressed in this study were formulated as,

i. To develop time series from January 2001 to December 2020 with meteorological drought indices (SPI & SPEI) and remotely-sensed vegetation index anomalies (NDVI-A) and NDWI-A) for the study area.
ii. To establish a root zone soil moisture time series from profile soil moisture measured across Twente region.
iii. To assess the behavior of drought indices with respect to the identification of the onset and frequency of droughts against the root zone soil moisture measurements over the Twente region.
iv. To explore the agreement between surface soil moisture as observed by the satellites and root zone soil moisture as measured in-situ across Twente.

The research questions investigated in the this research are,

i. How does drought progress over-time from the perspective of meteorological drought indices and remotely sensed vegetation index anomalies?
ii. What assumptions are needed for developing and computing reliable time series drought indices?
iii. How to determine the root zone soil moisture anomalies from soil profile measurements?
iv. How do the drought indices and root soil moisture anomalies compare over-time?
v. How do surface and root soil moisture measured across the Twente region compare to each other?

1.4. Research hypothesis

The research hypothesized that meteorological drought indices and remotely sensed indices could detect agricultural droughts as observed by soil moisture anomalies in the study area. To chieve this hypothesis, it was assumed that the time series meteorological indices (SPI and SPEI) would adequately indicate climatic anomalies in the study area using available rainfall and crop reference evapotranspiration data (1988-2020) from Twenthe, KNMI station. The use of remotely sensed vegetation index anomalies, followed the general assumption that there exists a relationship between the "greenness" estimated by satellite sensors and moisture conditions in a region (Di et al., 1994; Gutman, 1990; Ji & Peters, 2003). The use of anomalies was assumed to remove seasonal variations observed in vegetation as suggested by van Hateren

et al. (2021). The integral role of soil moisture in land processes was assumed to be an important variable in illustrating the climate- soil- vegetation- relationships in the hydrological cycle. An assumption in the study was moisture variability was as a function of natural climate variability, omitting irrigation inflows.

1.5. Conceptual framework of research

This research focused on the first two types of droughts, meteorological and agricultural droughts (highlighted in Figure 2). Meteorological drought indices (SPI and SPEI) and remote sensed vegetation index anomalies (NDVI-A and NDWI-A) were selected to quantify the drought events in the study area. SPI and SPEI were used as representatives of meteorological droughts and their complementarity in the parameters used to quantify drought, that is, precipitation (SPI) and water deficit (SPEI). The NDVI-A and NDWI-A observe chlorophyll content and leaf water content respectively. The drought indices were computed for two short time scales (16-day and monthly) to detect the shortest drought event as possible since drought is a function of time. These indices were compared against soil moisture anomalies to observe their sensitivity to soil variability.

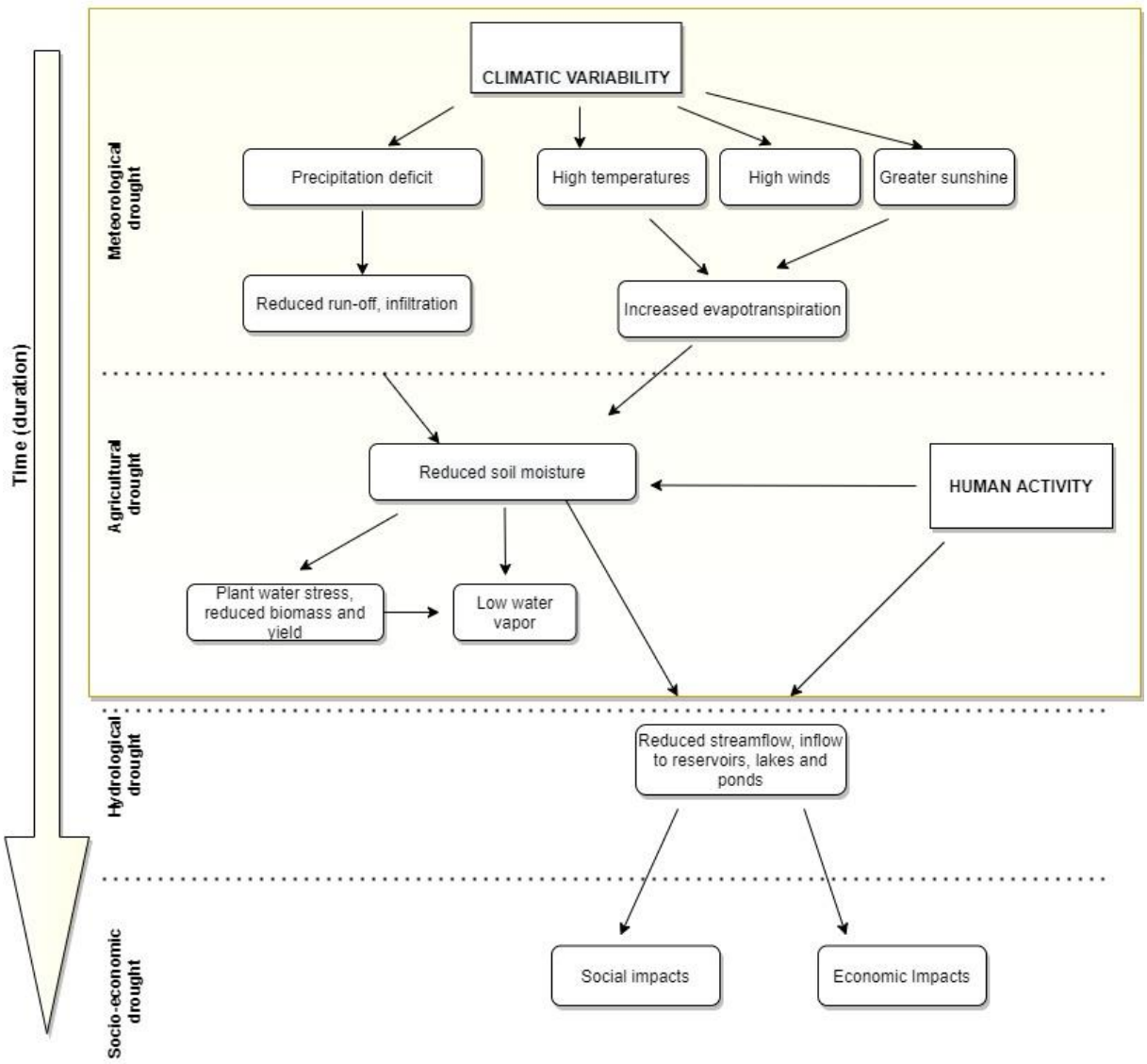

Figure 2: Propagation of drought through the hydrological cycle as a function of time. Adapted from "Seasonal Drought Prediction: Advances, Challenges, and Future Prospects" by Hao, Z., Singh, V. P., & Xia, Y. 2018. Copyright 2018 Blackwell Publishing Ltd

1.6. Thesis structure

This research is structured into six sections. **Section one** introduces the scientific background of the research, research problem, research objectives, research hypothesis and conceptual framework of the research. **Section two** focuses on the study area including the climate, the meteorological and soil measurements acquired from the region. **Section three** includes remote sensing data and processing of the products; **section four** discusses the different methods applied to come up with drought indices and methods of comparison. **Section five** consists of the results and discussion of results. **Section six** includes the conclusion and recommendation of the study.

2. STUDY AREA AND IN-SITU MEASUREMENTS

2.1. Twente region

Twente region is located in the Eastern part of the Netherlands in the Overijssel province (52° 06' N - 52° 30'N, 6° 15' E - 7° 05' E). The region is relatively flat with altitudes ranging between 3m to 85 m above sea level (Pezij et al., 2019). Pasture is the major vegetation on agricultural fields while a few fields grow corn, wheat, and potatoes (Van Der Velde et al., 2021). Soils in the region are sandy with more loamy soils (Buitink et al., 2020). Often, fields in low lying flat areas suffer from stagnant water during wet seasons in winter and extreme rainfalls in summer (Van Der Velde et al., 2021). The Twente soil monitoring network is found in the region and encompasses about twenty-two soil moisture stations as indicated in Figure 3.

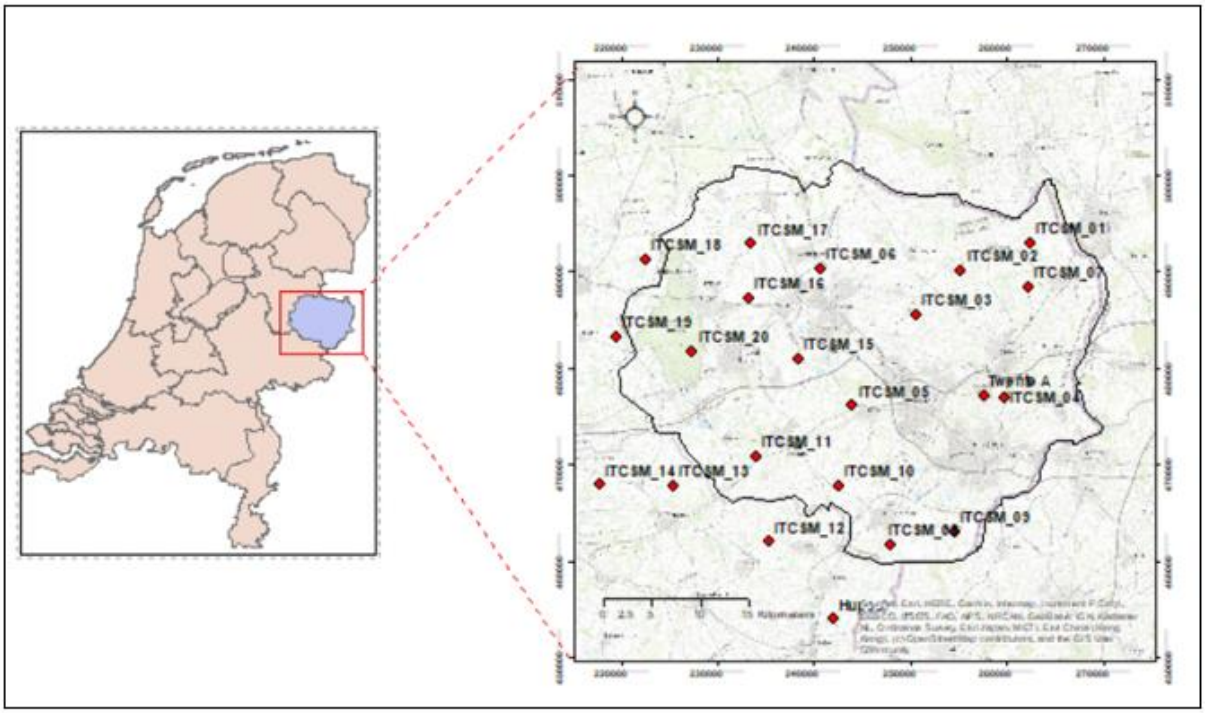

Figure 3: Study area (a) Left side: Netherland's map indicating the location of Twente region (b) Right side: Twente region indicating Twente soil monitoring network (red marks)

The climate of the region is temperate marine (Hendriks et al., 2014). The winter and summer seasons tend to be mild and wet with a few extremes of below -10 ºC and above 30 ºC in winter and summer respectively (Van Der Velde et al., 2021). For better understanding of the prevailing climatic conditions in the region in reference to the long-term normal conditions (33 years), Figure 4 (a) illustrates the long-term monthly average rainfall and reference crop evapotranspiration (ET_{ref}) over (1988-2020). Figure 4 (b) illustrates the variations in the climatic conditions for the recent years (2018-2020).

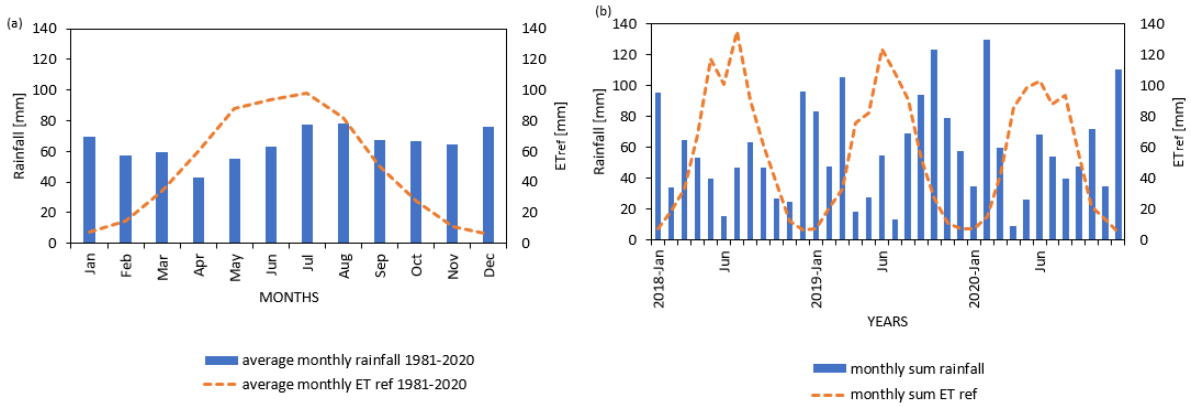

Figure 4: (a) average monthly rainfall and average monthly crop reference evapotranspiration *(ET*$_{ref}$*)* for the period 1988-2020 (b) monthly sum rainfall and monthly sum *ET*$_{ref}$ for the period 2018-2020, derived from meteorological observations performed at KNMI's Twenthe automated weather station.

2.2. Meteorological measurements

In this study, the meteorological variables used for the computation of time series meteorological drought indices were daily measured precipitation (resolution 0.1 mm) and daily calculated crop reference evapotranspiration *(ET*$_{ref}$*)* (resolution 0.1 mm) from the automated weather station of the Royal Netherlands Meteorological Institute (KNMI). Weather data used for the calculation of crop reference evapotranspiration *(ET*$_{ref}$*)* include daily mean temperature (°C), latitude of the station, daily mean surface air pressure (hPa) and daily sunshine duration (0.1h), which are all measured at the station or known. Long term historical data of meteorological variables were accessible from the KNMI website after data quality checks (source: https://www.knmi.nl/nederland-nu/klimatologie). Thirty-three-year record data was derived from KNMI Twenthe station. The data is acquired in 0.1 mm hence scaled to 1_mm for the entire time series before further analysis.

The KNMI stations being sparsely located, limited the study to one weather station. Moreover, the long-term average rainfall (1981-2020) received in the region in different months indicated that the rainfall does not vary significantly across the study area (see Figure 5).

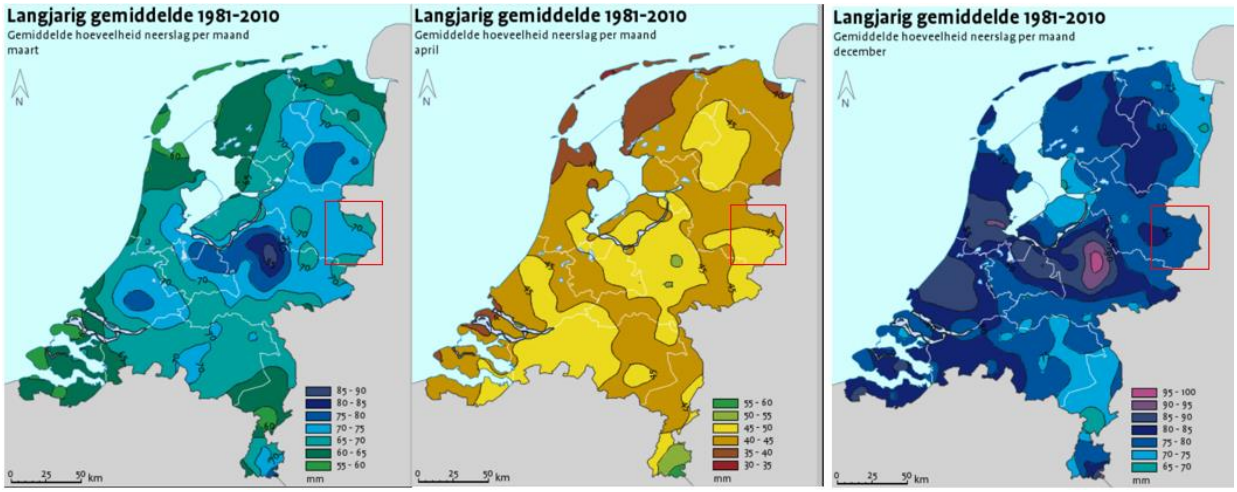

Figure 5: Average long term monthly precipitation (1981-2010) for sample months (March, April & December respectively). Red box illustrates the study area.

source: https://www.meteo-julianadorp.nl/Klimaatatlas/Klimaatatlas-Neerslag.html

Table 2 Summary of KNMI station meteorological data

Meteorological variable	**Type of data**	**Temporal resolution**	**Period**
Precipitation (mm/day)	Measured	Daily	1988 - 2020
Crop reference potential evaporation (mm/day)	Calculated	Daily	1988 - 2020

2.3. Soil moisture profile measurements

In - situ soil profile measurements were acquired from the Twente soil monitoring network that has been previously used as a validation site for satellite estimates (Van Der Velde et al., 2021). The soil profile measurements record volumetric soil moisture (θ) [m^3_{water}/m^3_{soil}] and temperature [°C] at nominal depths of 5-cm, 10-cm, 20-cm, 40-cm, and 80-cm (Van Der Velde et al., 2021). The soil moisture sensors are spread over different vegetation cover with majority of the sensors installed on pasture / grass, a few in corn fields and one station in a forest. The forest location was terminated in 2017. The temporal resolution of the data is 15 minutes as recorded by the Decagon EM50 ECH2O data loggers (Dente et al., 2011). The available soil moisture observations were for the period 2015- 2020 for about Twenty soil moisture stations. The data was acquired from the ITC Water department as processed and calibrated data.

2.3.1. Root zone soil moisture

The data records for the soil moisture stations had several gaps. Some stations had incomplete measurements of (5-cm, 10-cm) profile measurements. Majority of the stations had complete measurements up to 40-cm and these are the stations that their data records were used in the study (twelve stations in 2015, & seventeen stations from 2016 to 2020). The availability of data of up to 40-cm made this the preferred root depth. Moreover, Pezij et al., (2019) determined the root zone depth for different vegetation types in Twente region for both summer and winter periods as varying between 0.20-m in winter and 0.40-m in the summer period for grass and between 0.10-m in winter and 0.40-m during summer for corn fields.

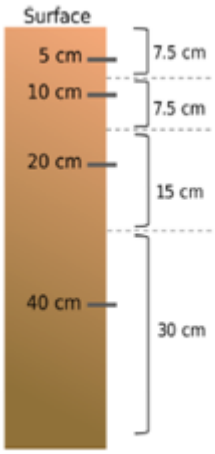

Figure 6: A schematic diagram showing the installation setup at each soil moisture station and the depth at which the root zone was calculated (40cm). Adapted from "Root zone soil moisture estimation with Random Forest." By Carranza, C., Nolet, C., Pezij, M., & van der Ploeg, M. 2021, Journal of Hydrology, Copyright 2021 by Elsevier B.V.

The root zone soil moisture was calculated based on Carranza et al., (2021) root zone moisture estimation method of using the zone-weighted depth-averaged values of the soil profile measurements and associated soil thickness, given by the Eq. (1). The method took the midway distance between the adjacent measurement points in the soil profile (see figure 5).

$$\theta_{rz} = \frac{\sum_{j=1}^{n} \theta_j \Delta_{Zj}}{z} \qquad \text{Eq 1}$$

Where θ_{rz} is the root zone soil moisture, θ_j is the volumetric water content (m^3/m^3) for the measurement depth j (m), Δ_{Zj} (m) is the thickness of the soil associated with the measurement depth, and z (m) is the total averaging depth of the profile, in this case 0.40m.

3. REMOTE SENSING DATA

3.1. Mission and instrument

The vegetation indices used for this study were acquired by the MODIS (MOderate Resolution Imaging Spectroradiometer) instrument onboard both the Terra (EOS AM) and Aqua (EOS PM) satellites. Terra satellite was launched by the end of 1999 whereas Aqua satellite was launched in 2002. MODIS has a temporal resolution of 1 to 2 days, acquiring data in 36 spectral bands https://modis.gsfc.nasa.gov/data/ These spectral bands provide data in three spatial resolutions 250 m, 500 m, and 1 km (Lindsey & Herring, 1990). The high spatial resolutions are seen as an improvement over the AVHRR sensor which provides 1 km resolution local area coverage and 4 km resolution global area coverage (Huete et al., 1997). MODIS offers surface reflectance data products that are an estimate of ground observations in absence of atmospheric interference, and among the products are the vegetation indices products (Vermote et al., 2015).

3.2. Data Products

3.2.1. Time series NDVI

One of MODIS vegetation indices products is the NDVI data product that is a 16-day composite. In this study, MODIS VI NDVI (MOD13A1) data products were used, generated from two 8-day composite surface reflectance of TERRA MODIS red and near infrared bands at 500m spatial resolution (Didan et al., 2015). The product is corrected for atmospheric conditions such as gases, aerosols, and Rayleigh scattering (Vermote et al., 2011). The time series for each year started at 001 and ends at 353, with an interval of 16 days. The equation used to obtain the 16-day composite is

$$\text{NDVI} = \frac{\rho_{\text{red}} - \rho_{\text{NIR}}}{\rho_{\text{red}} + \rho_{\text{NIR}}} \qquad \text{Eq 2}$$

Where ρ_{red}, and ρ_{NIR} are MODIS band 1 (620 – 670 nm) and band 2 (841-876 nm) respectively.

NDVI data for the study area was acquired from the Land Processes Distributed Active Archive Centre using the AppEARS tool that allows for easy access to MODIS data products using point sample of geographic co-ordinates or area sample of vector polygon (shapefiles) https://lpdaac.usgs.gov/tools/appeears/. Soil moisture geographic co-ordinates (22 points) from the Twente soil moisture network were used to acquire data as point samples over the period from 2001 to 2020.

The AppEARS tool allowed for the specification of the data format and projection before data acquisition, that is available in GeoTIFF format and geographic projection (datum: WGS 84). The data was linearly scaled with NDVI values ranging between -1 to 1.

3.2.1.1. NDVI Data processing

Alongside the NDVI data product, is the Quality assessment metadata that was used to filter and omit data values captured with the lowest quality, that is, pixels produced under cloudy conditions. De Oliveira & Epiphanio, (2012) suggested the use of these Quality assessment (QA) in pre-processing NDVI to check for errors in the MODIS data products before further analysis.

The NDVI data used for research did not consider smoothing techniques since further processing (averaging to spatial mean) of the point-derived data was further done and this would minimize inherent point skewed data. Rahimi, (2020) pointed out that the Harmonic Analysis of Time Series (HANTS) (Roerink et al., 2000; Wit & Su, 2005), a commonly used smoothing method, had limitations of not retaining the actual NDVI values observed at given observation dates. Tian et al. (2015) argued that averaging NDVI values for a region reduces small scale errors by balancing them out leaving room for detection of major errors caused by sensor differences or sensor shifts. Moreover, many data smoothing procedures are more appropriate when assessing phenological indicators such as the start and end and length of the growing season (Kross, 2005).

As a result, actual observations were used to obtain the spatial means NDVI of the study area. To obtain spatial mean NDVI for the study area, an average over the soil moisture point NDVI estimates was computed for each 16-day DOY observation. Aggregation by average method on all land cover types for an entire region was applied by Mennis, (2001) to get spatial mean. For better understanding of the NDVI variations over the years, average 16-day NDVI timeseries over the period 2001-2020 was plotted (see Fig. 4(a)). To derive monthly NDVI values, average of two 16-day DOY observations according to the date of capture was done and the average monthly NDVI timeseries was plotted (2001-2020) (see Fig. 4 (b)).

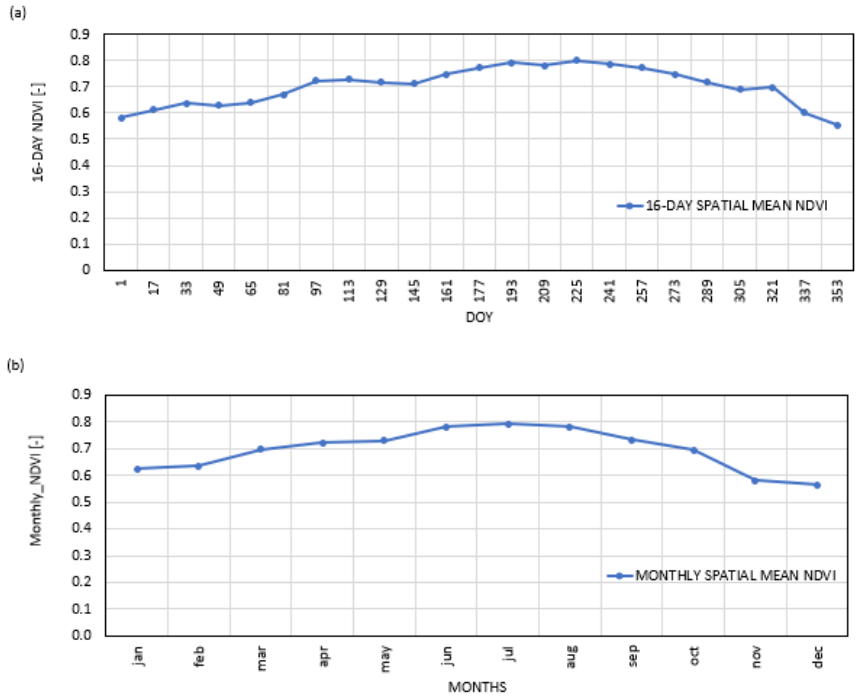

Figure 7: (a) 16-day spatial mean for NDVI timeseries from 2001-2020 plotted against the Day of the Year (DOY), (b) monthly spatial mean for NDVI timeseries from 2001-2020, derived from MODIS surface reflectance products (MOD13A1) version 6 collection

3.2.2. Time series NDWI

Long term NDWI datasets are not readily available. This necessitated the calculation of the index based NIR (band 2) and SWIR (band 6) surface reflectance bands from MODIS product (MOD09A1) Version 6 collection. From the Land Processes Distributed Active Archive Centre using the AppEARS tool https://lpdaac.usgs.gov/tools/appeears/, geographic co-ordinates from the Twente soil moisture network were used to acquire data as point samples from 8-day NIR and 8-day SWIR bands at 500m. Unlike the 16-day composite NDVI product, the 8-day surface reflectance products were the best observed estimate within an 8-day period. The best product was one taken with a low view angle, cloud free or minimal cloud and cloud shadow (Roger et al., 2011).

3.2.2.1. NDWI Data processing

The NDWI data products from MOD09A1 had a Quality assessment metadata also, that was used to filter and omit the lowest quality data values (those captured under cloudy conditions). The two datasets (8-day NIR and 8-day SWIR bands) containing 22 time series (number of soil moisture station points) for the period 2001-2020 each, were used for the calculation of the NDWI to obtain the 8-day NDWI values using Equation 4.

$$NDWI = \frac{\rho NIR - \rho SWIR}{\rho NIR + \rho SWIR} \quad \text{Eq. 3}$$

Where ρ_{NIR}, and ρ_{SWIR} are MODIS bands 2 (841-876 nm) and band 6 (1628-1652 nm) respectively. The NDWI data values had a range of -1 to 1. An average of two calculated 8-day NDWI observations was done to obtain 16-day NDWI time series for the Twente region and subsequent average of two 16-day NDWI calculations to obtain monthly NDWI values. To obtain spatial mean NDWI for the study area, an average over the soil moisture point NDWI estimates was computed for each 8-day, 16-day DOY and monthly observation and plotted for the period 2001-2020 (see Figure 9)

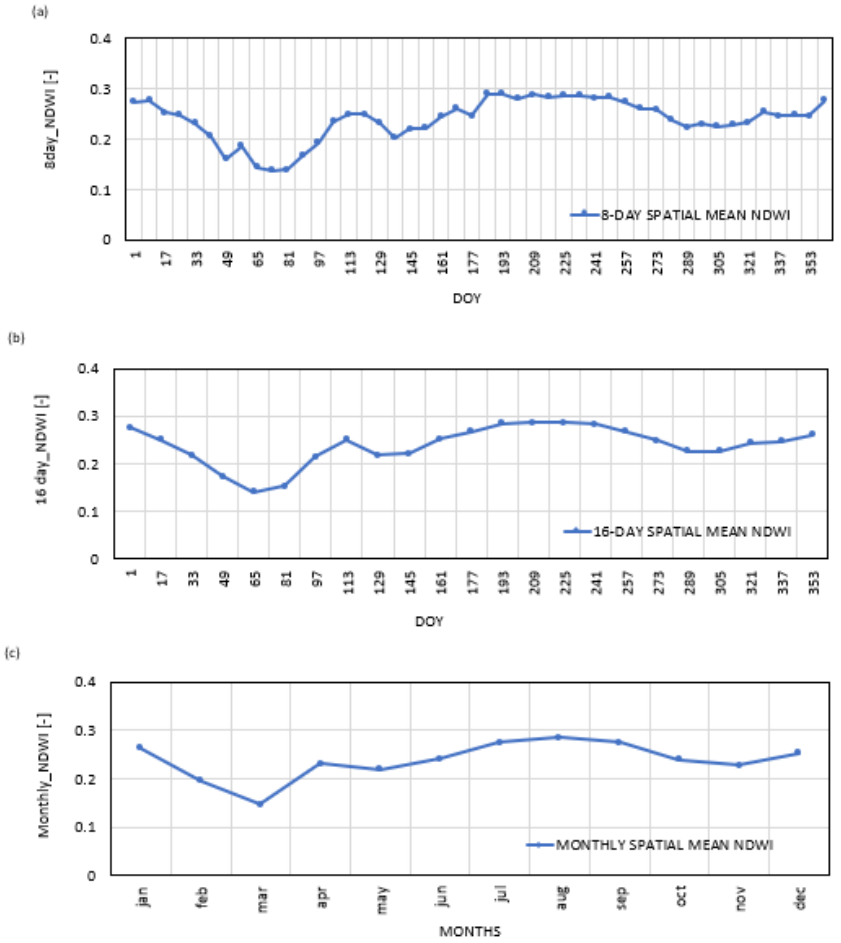

Figure 8: (a) 8-day spatial mean for NDWI timeseries from 2001-2020 plotted against 8-day Day of the year (DOY), (b) 16-day spatial mean for NDWI timeseries from 2001-2020 plotted against 16-day DOY & (c) monthly spatial mean for NDWI timeseries from 2001-2020, derived from MODIS surface reflectance products (MOD09A1) version 6 collection

4. METHODS

4.1. Standardized Precipitation Index (SPI)

To compute the Standardized Precipitation Index (SPI), rainfall records of more than 30 years (climatology) are essential. This study used thirty-three-year daily precipitation data (1988 – 2020). 16-day and monthly precipitation time series were fitted to a gamma probability distribution function (PDF). The gamma was recommended as the most suitable PDF for fitting rainfall at various timescales by Lloyd-Hughes & Saunders, (2002) who tested several PDFs (gamma, log-normal and normal) using a Kolmogorov-Smirnov Test (K-S test) and gamma showed the best fit. The K-S test (Chakravarti et al., 1967) is a non-parametric statistical fit test that compares hypothetical PDF (e.g., gamma) with the empirical PDF, generated by the data. The hypothetical PDF that best fits the empirical PDF is most suitable (Chakravarti et al., 1967). (see Figure 9.)

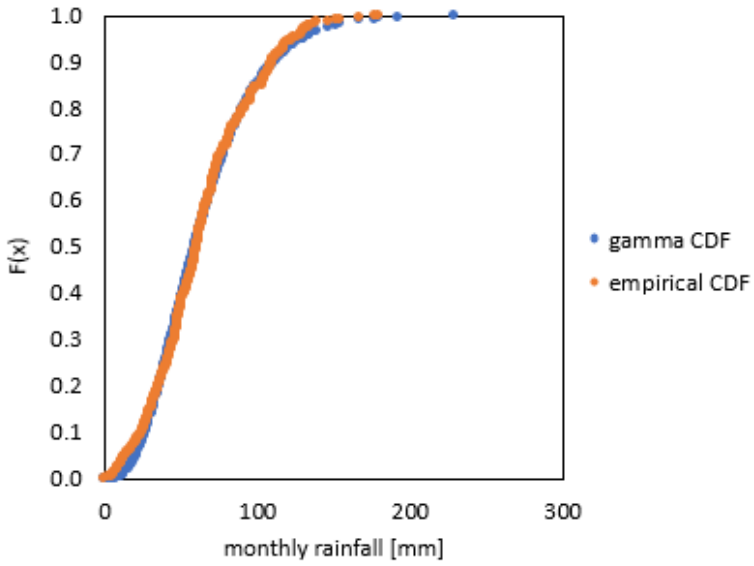

Figure 9: Scatter plot indicating gamma CDF fitness to monthly rainfall empirical CDF

The gamma PDF was given by the equation:

$$g(x) = \frac{1}{\beta^{\alpha}\Gamma_{(\alpha)}} x^{\alpha-1} e^{x/\beta} \quad for\ x > 0 \qquad \text{Eq 4}$$

Where $\alpha > 0$ is a shape parameter, $\beta > 0$ is a scale parameter, $x > 0$ is the amount of precipitation and $\Gamma(\alpha)$ is the gamma function. The two timeseries of 16-day precipitation and monthly precipitation were uploaded into a math program, EasyFit professional version 5.0 used for fitting data to their distributions (source: https://easyfit.informer.com/5.5/). -The estimation of the α and β parameters is done by the

program based on the Maximum likelihood estimation (Genidy, 2020). The fitted gamma PDF is used to calculate the cumulative distribution function (CDF) using the equation:

$$G(x) = \frac{1}{\hat{\beta}^{\hat{\alpha}}\Gamma(\hat{\alpha})}\int_0^x t^{\hat{\alpha}}\, e^{-x/\hat{\beta}}\, dx \qquad \text{Eq 5}$$

The inverse normal function was applied to the CDF to obtain standardized normal distribution of SPI values with a mean zero and standard deviation of one (Guttman, 1998; Sepulcre-Canto et al., 2012).

4.2. Standardized precipitation and Evaporation Index (SPEI)

The computation of SPEI involved use of precipitation and the crop reference evapotranspiration *(ET_{ref})* data. The acquired ET_{ref} data is calculated using a radiation-based Evapotranspiration method, the Makkink formula, that incorporates incoming shortwave radiation and average daily temperatures. The crop reference evapotranspiration *(ET_{ref})* is defined as the "atmospheric evaporative demand of grass as the hypothetical reference crop surface and its independent of the crop type or crop development" (Allen et al., 1998, p. 7). The ET_{ref} is majorly driven by radiation, temperature, humidity and windspeed at different latitudes (Peng et al., 2018) and these variables captured by the Makkink equation expressed as:

$$ET_{ref} = 0.65 \,.\, \frac{\theta}{\theta+\gamma} \,.\, \frac{s\downarrow_{day}}{\lambda * \rho} \qquad \text{Eq 6}$$

Where ET_{ref} is the Makkink reference evaporation (mmd^{-1}), θ the slope of the curve of saturation water vapor pressure ($kPa^{o}\ C^{-1}$) that is derived from the mean daily temperature, γ the psychometric constant ($kPa^{o}\ C^{-1}$), $s\downarrow_{day}$ the daily incoming shortwave radiation ($Jm^{-2}d^{-1}$) and ρ the bulk density of water, i.e. 1000 kgm^{-3} (Hiemstra & Sluiter, 2011).

Steps of computing SPEI index are similar to the SPI computation procedure. Thirty-three-year daily precipitation and daily crop reference evapotranspiration *(ET_{ref})* (1988-2020) were summed up to 16-days and monthly timescales. The water deficits (D) were computed, given by,

$$D_i = P_i - ET_{ref} \qquad \text{Eq 7}$$

Where D_i is water deficit at timescale i (16-days / monthly), P_i is precipitation at timescale i and ET_{ref} is the crop reference evapotranspiration at timescale i. The water deficit time series (D) from each time scale (16-day and 1 month) were then fitted into a log logistic distribution which has been recommended by S. M. Vicente-Serrano et al. (2010) (see Figure10.)

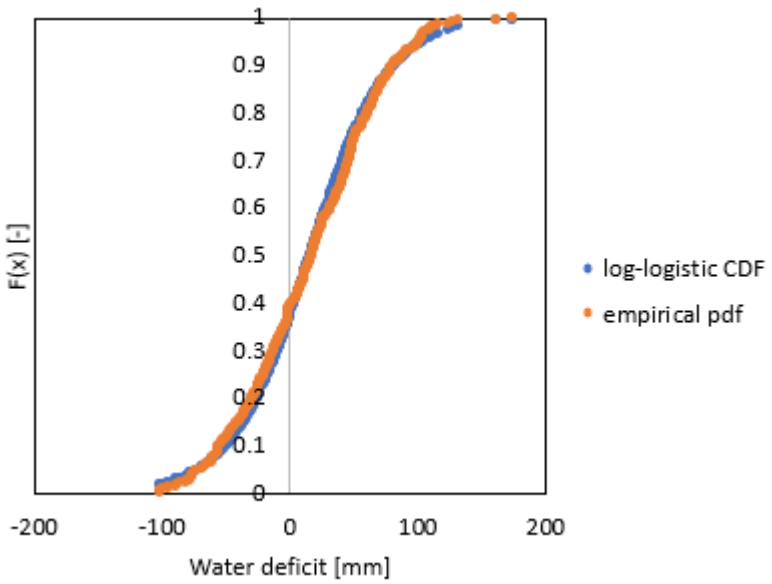

Figure 10: Scatter plot indicating log-logistic CDF fitness to the monthly water deficit empirical CDF

The Log-logistic distribution, which is a three-parameter distribution can account for negative values and is given by:

$$f(x) = \frac{\beta}{\alpha}\left(\frac{x-\gamma}{\alpha}\right)^{\beta-1}\left[1+\left(\frac{x-\gamma}{\alpha}\right)^{\beta}\right]^{-2} \quad \text{Eq 8}$$

where x can take values in a range $(\Upsilon > x > \infty)$, Υ is the parameter of origin and x can take any value including negative values found in water deficit values (S. M. Vicente-Serrano et al., 2010). The parameters of the distribution were then retrieved from the EasyFit program using the Maximum Likelihood Estimation. Results from the program were pointed out to be quantifiable in a study that compared parameter estimation of log-logistic distribution using the software and using an algorithm of percentile roots (Genidy, 2020). The CDF of the log-logistic distribution is given by:

$$F(x) = \left[1+\left(\frac{\alpha}{x-\gamma}\right)^{\beta}\right]^{-1} \quad \text{Eq 9}$$

Where $\alpha, \beta,$ and Υ are the scale, shape, and origin parameters for the water balance series (D) $(\Upsilon > D > \infty)$. The SPEI index was then calculated as standardized values of F(x) using the classical approximation of Abramowitz and Irene (1970) that has been recommended in many studies (Pei et al., 2020; S. M. Vicente-Serrano et al., 2010).

$$SPEI = W - \frac{C_0 + C_1 W + C_2 W^2}{1 + d_1 W + d_2 W^2 + d_3 W^3} \quad \text{Eq 10}$$

where,

$$W = \sqrt{-2\,ln(P)}\ for\ P \leq 0.5 \quad \text{Eq 11}$$

P is the probability of exceeding a determined water balance (D) value, $P = 1 - F(x)$. Where if $P > 0.5$, P is replaced by $1 - P$ and the sign of the resultant SPEI is reversed. The constants used in the equation are C0 = 5 2.515517, C1 = 5 0.802853, C2 = 0.010328, d1 = 1.432788, d2 = 0.189269, and d3 = 0.001308. To quantify the severity of drought conditions, SPEI values were put to similar categories as SPI values (S. M. Vicente-Serrano et al., 2006; 2010) (see Table 1).

4.3. Vegetation indices anomalies

4.3.1. NDVI Anomaly (NDVI-A)

The NDVI anomaly (NDVI-A) is derived from comparing the current NDVI value with the long-term mean NDVI for a given timestep (Anyamba & Tucker, 2012). In the research, to derive the NDVI anomalies, the long-term mean NDVI and standard deviation at both timesteps (16-day and monthly) were computed for the whole period (2001-2020). Standardized NDVI anomalies were calculated following the procedure by Udelhoven et al. (2009).

$$NDVI_{anomaly\,i} = \frac{NDVI_{mean\,i} - \overline{NDVI\,i}}{NDVI_{\sigma\,i}} \quad \text{Eq 12}$$

Where $NDVI_{anomaly,}$ is the NDVI anomaly for the timestep i (16-day, or monthly) and $NDVI_{mean}$ is the spatial mean NDVI over the study area at timestep i (16-day, or monthly) and $\overline{NDVI}$ is the long-term mean NDVI and $NDVI_{\sigma}$ is the long-term standard deviation for corresponding timestep i (16-day, or monthly). The NDVI anomalies were then classified according to SPI /SPEI classification scheme in Table 1 since the anomalies were calculated using a similar normalization procedure used in SPI and SPEI computation.

4.3.2. NDWI Anomaly (NDWI-A)

To derive NDWI anomalies at 16-day and monthly timestep, the long-term mean NDWI and standard deviation were first computed for the period (2001 - 2020) for both timesteps. The NDWI anomalies were then calculated using the equation,

$$NDWI_{anomaly\,i} = \frac{NDWI_{mean\,i} - \overline{NDWI\,i}}{NDWI_{\sigma\,i}} \quad \text{Eq 13}$$

Where $NDWI_{anomaly,}$ is the NDWI anomaly for the timestep i (16-day, or monthly) and $NDWI_{mean}$ is the spatial mean NDWI over the study area at timestep i (16-day, or monthly) and $\overline{NDWI}$ is the long-term mean NDWI and $NDWI_{\sigma}$ is the long-term standard deviation for corresponding timestep i (16-day, or monthly). Similar to the NDVI anomalies, the drought categories were categorized according to SPI & SPEI classification scheme (see Table 1.)

4.4. Soil moisture anomalies

The soil moisture anomalies were grouped into surface soil moisture anomalies (θ_{sm} – A) and root zone soil moisture anomalies (θ_{rz} - A). These anomalies were calculated as a deviation from the mean of the six-year soil moisture records at the two timescales (16-day, monthly). Due to the limitation of in-situ measurements in providing long-term data, only six-year data was available for determining soil moisture anomalies. The mean and the standard deviation for the full period (2015-2020) were first computed and Equation 15 used to compute the surface soil moisture anomalies and Equation 16 to compute the root zone soil moisture anomalies.

$$\theta_{sm} - A_i = \frac{\theta_{sm\,i} - \overline{\theta_{sm\,i}}}{\theta_{sm}\sigma\,i} \qquad \text{Eq 14}$$

Where $\theta_{sm} - A$ is the surface soil moisture anomaly for the timestep i (16-day, or monthly), $\theta_{sm\,i}$ is the surface soil moisture for the timestep i (16-day, monthly), $\overline{\theta_{sm\,i}}$ is the long-term average surface soil moisture and $\theta_{sm}\sigma\,i$ is the standard deviation surface soil moisture for corresponding timestep i (16-day, or monthly).

$$\theta_{rz} - A_i = \frac{\theta_{rz\,i} - \overline{\theta_{rz\,i}}}{\theta_{rz}\sigma\,i} \qquad \text{Eq 15}$$

Where $\theta_{rz} - A$ is the root zone soil moisture anomaly for the timestep i (16-day, or monthly), $\theta_{rz\,i}$ is the root zone soil moisture for the timestep i (16-day, monthly), $\overline{\theta_{rz\,i}}$ is the long-term average root zone soil moisture and $\theta_{rz}\sigma\,i$ is the standard deviation root zone soil moisture for corresponding timestep i (16-day, or monthly). The soil moisture anomalies were grouped according to SPI & SPEI classification scheme (see Table 1.)

4.5. Description of analysis methods

4.5.1. Trend Analysis

In this study, trend analysis was done using the Mann-Kendall test (Kendall, 1948; Mann, 1945) which is a non-parametric statistical method that looks at the correlation between ranks and sequencies in a data series. It has been used in trend detection of climatic variables (Karmeshu, 2012). A significance level of 5% (p = 0.05) has been applied in identifying trends in drought indices (Alsafadi et al., 2020; Hui-Mean et al., 2018). The trend test is depended on the value of p that is the basis of the two hypothesis, null hypothesis suggests that p ≥0.05, there is no existence of a trend in data and alternative hypothesis suggests the existence of a trend when p ≤ 0.05. The Mann-Kendall test (S) considers n data points of a time series given by,

$$S = \sum_{i=1}^{n-1} \sum_{j=i+1}^{n} sgn(X_j - X_i) \quad \text{Eq 16}$$

$$sgn(X_j - X_i) = \begin{cases} 1 & if\ X_j - X_i > 0 \\ 0 & if\ X_j - X_i = 0 \\ -1 & if\ X_j - X_i > 0 \end{cases} \quad \text{Eq 17}$$

Where $X_j\ and\ X_i$ are two subsets of data where i, = 1,2,3, …., $n-1$ and $j = i+1, i+2, i+3, \ldots, n$ $X_j\ and\ X_i$ can be monthly precipitation /drought index or 16 days precipitation /drought index values in years j and i where $j > i$ respectively. The use of programming language, python, facilitated the testing of the data series using the pymannkendall library (Hussain & Mahmud, 2019).

4.5.2. Correlation Analysis

To statistically analyse the relationship between the meteorological drought indices (SPI & SPEI), vegetation anomalies (NDVI-A & NDWI-A), and the root zone soil moisture anomalies, Pearson correlation coefficient (R) was used. The correlation coefficient was used to measure linear association between two continuous variables where a high value depicts a strong association and a low value depicts the lack of association (USGS, 2020). The correlation coefficient was also calculated at different time lags.

$$R_{xy} = \frac{\sum_{i=1}^{n}(x_i - \bar{x})(y_i - \bar{y})}{\sqrt{\sum_{i=1}^{n}(x_i - \bar{x})^2}(y_i - \bar{y})^2} \quad \text{Eq 18}$$

Where R_{xy} is the Pearson correlation coefficient of two datasets x and y of n are the number of data points. x can be a meteorological or vegetation drought indices series and y is soil moisture anomalies series respectively.

Many investigations have used the correlation analysis in drought analysis to find the relationship between vegetation drought indices and soil moisture (West et al., 2018), between surface soil moisture anomalies and SPI at various timescales (Spennemann et al., 2015).

To test for the significance of the correlation coefficient (R), the probability value (p-value) was used as computed from a t-test (which gives information on the strength of the linear relationship) (Greenland et al., 2016). To p-value ranges from 0 to 1, where values closer to zero indicate that (R) is statistically significant and a larger p-value indicates non-significance (Illowsky & Dean, 2021). In this research, at 5% significance level, p values ≤ 0.05 indicated that the linear association (R) was significant and p values ≥ 0.05 suggested that (R) was not significant. The T-test is given by,

$$t = \frac{R\sqrt{n-2}}{1-R^2} \qquad \text{Eq 19}$$

Where R is the Pearson's correlation co-efficient, R^2 is the coefficient of determination and n number of data points.

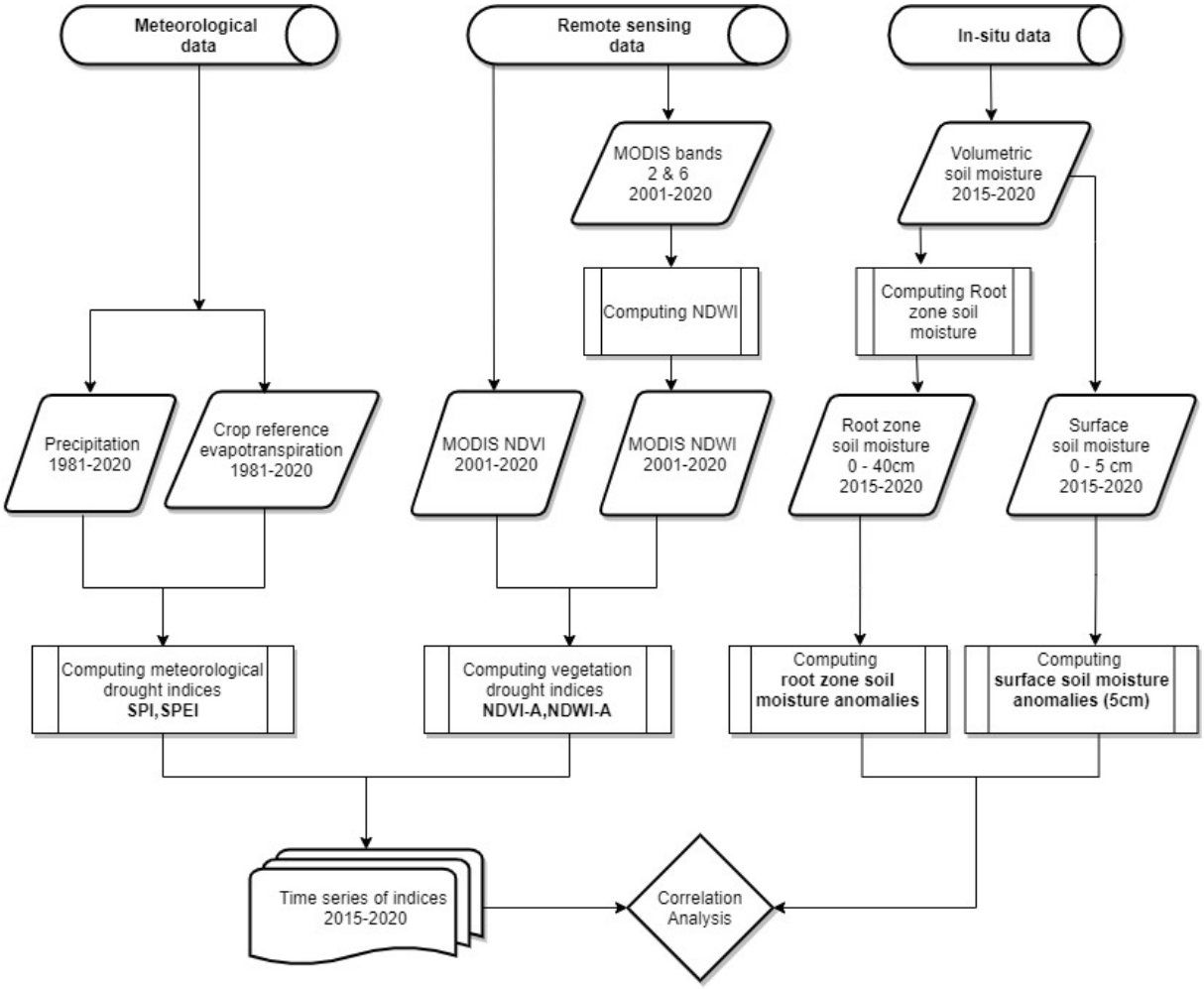

LEGEND

SPI	Standardized precipitation index
SPEI	Standardized precipitation evapotranspiration index
NDVI	The Normalized Difference Water Index
NDWI	The Normalized Difference Water Index
NDVI-A	NDVI Anomaly
NDWI-A	NDWI Anomaly

Figure 11: Flow chart of the Methods used in the study

5. RESULTS AND DISCUSSION

In this chapter, the results of the study are discussed. **Section 5.1** discusses the temporal evolution of meteorological drought as quantified by SPI and SPEI at 16-day and monthly timescales. In addition, further analysis is done to detect the frequency and severity of meteorological drought events for the period 2001 to 2020. **Section 5.2** discusses the temporal evolution of agricultural drought as quantified by vegetation index anomalies (NDWI-A and NDVI-A) at 16-day and monthly timescales. Analysis is also done detect the frequency and severity of the agricultural drought events over 2001-2020. **Section 5.3** discusses the temporal evolution of soil moisture anomalies (surface, $\theta_{sm} - A$ and root zone, $\theta_{rz} - A$) for the period 2015 to 2020. A comparison analysis using Pearson's correlation coefficient (R) is done to show the relationships between the drought indices and soil moisture anomalies at 16-day and monthly timescales. **Section 5.4** shows an overview of how drought indices quantified the 2018 drought. **Section 5.5** outlines the assumptions / limitations in the development of the drought indices (meteorological, agricultural and soil moisture anomalies)

5.1. Meteorological drought indices

Standardized precipitation index (SPI) and Standardized precipitation evapotranspiration index (SPEI) are the meteorological drought indices used for quantifying drought in the last twenty years (2001 – 2020). Due to their multi-temporal characteristic, both indices were computed according to 16-days and monthly timescales to capture drought events of different magnitudes / severity and their frequency in a short-term duration. Drought commences when the SPI / SPEI value goes below zero to negative values and ends when the values approach zero and progress towards positive values (non-drought).

5.1.1. Temporal evolution of meteorological drought

Figure 12 illustrates the variations in 16-day SPI and SPEI for the period (2001 – 2020). Further variations of monthly SPI and monthly SPEI are illustrated in Figure 13.

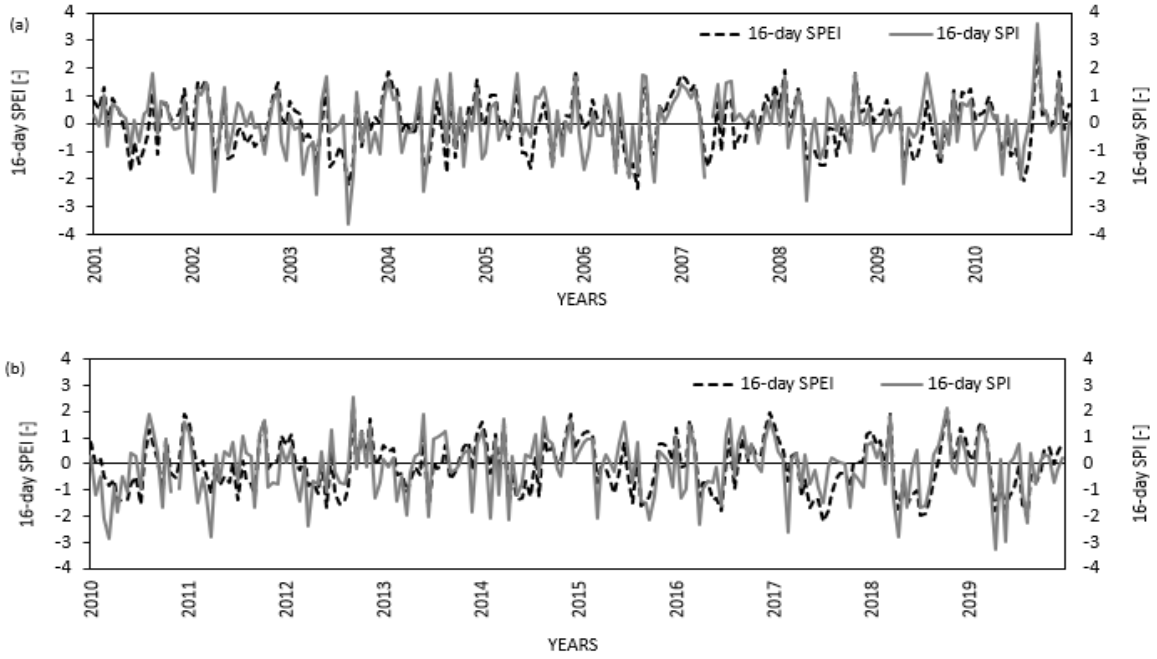

Figure 12: Temporal variations of 16-day SPI and SPEI timeseries over (a) 2001-2010 & (b) 2011– 2020.

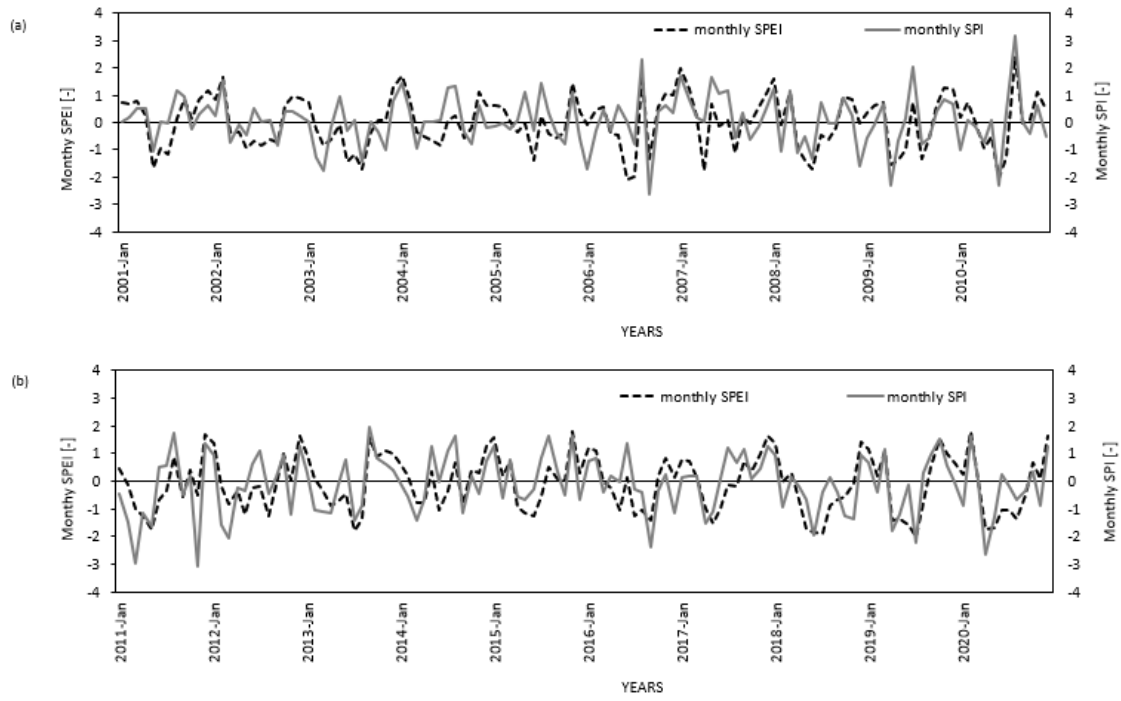

Figure 13: Temporal variations of monthly SPI timeseries and monthly SPEI timeseries over (a) 2001 – 2010 & (b) 2011– 2020.

Based on Figure 12, the 16-day SPI and SPEI show similarity of high fluctuations in identifying drought and non-drought events. This explains the detection of the slightest precipitation deficits within 16-days. A high coefficient of variation in rainfall and (ET_{ref}) at 16-day shown in Table 3 below, supports the

observed fluctuations. The indices illustrate differences in their peaks indicating differences in the magnitude / severity of the drought events they identify. A high non-significant correlation, R of 0.76, p (1.00) is yielded between the two indices at 16-day timescale. These results are in agreement with Stagge et al. (2014) who found that correlation of SPEI with SPI was in the range of (R of 0.65–0.98).

Based on Figure 13, the monthly SPI and SPEI illustrate a similar pattern in the detection of drought (below zero) and non- drought conditions (above zero) with minimal fluctuations compared to 16-day SPI and SPEI. A high non-significant correlation, R of 0.710, p (1.00) is yielded between monthly SPI and monthly SPEI. The differences in the magnitude of droughts quantified is slightly lower than in 16-day indices. This can be explained by a lower coefficient of variation in the monthly sum rainfall as the key driver of drought shown in Table 4. Pei et al., (2020) suggested that minimal fluctuations in monthly SPI and SPEI, are an indication of a long - term change characteristics of drought in response to climate anomalies of a month that are not observed in shorter timescales of 16 days.

Table 3: Statistical summary of 16-day sum rainfall and sum (ET_{ref}) in Twente region using thirty-three-year climatological data (1988-2020)

	16 - day sum rainfall	**16 - day sum (ET_{ref})**
Mean [mm]	33.87	25.95
Std [mm]	23.61	18.63
Coefficient of Variation (CV)	0.70	0.72

Table 4: Statistical summary of monthly sum rainfall and monthly sum ETo in Twente region using thirty-three-year climatological data (1988-2020)

	Monthly sum rainfall	**Monthly sum (ET_{ref})**
Mean [mm]	34.39	47.79
Std [mm]	65.26	35.13
Coefficient of Variation (CV)	0.53	0.73

5.1.2. Frequency of meteorological drought events and their degree of severity

Drought frequency is taken as the number of events identified within a certain category of severity over the total number of SPI /SPEI values (Nanzad et al., 2019). The levels of severity are determined using the drought classification categories of SPI and SPEI whereby, the negative values are grouped into moderately dry (≤ -1), very dry (≤ -1.5) and extremely dry (≤ -2.0) events. Oliveira-Júnior et al. (2018) also used this truncation level of drought events (≤-1) to evaluate drought severity using SPI.

Table 5: Summary of the degree of severity and frequency of drought events as identified by SPI and SPEI at both 16-day and monthly timescales over the period 2001-2020 for the Twente region

Meteorological drought indices		Moderately dry	Severely dry	Extremely dry
16-day SPI	Mean	-1.217	-1.**747**	**-2.505**
	Std dev	0.188	0.143	0.429
	Frequency [%]	7.7	5.5	5.0
16-day SPEI	Mean	-1.249	-1.656	-2.176
	Std dev	0.123	0.138	0.120
	Frequency [%]	12.3	7.0	1.1
Monthly SPI	Mean	-1.228	-1.701	**-2.514**
	Std dev	0.172	0.152	0.335
	Frequency [%]	10.0	2.9	3.8
Monthly SPEI	Mean	-1.228	-1.742	-2.073
	Std dev	0.149	0.134	0.01
	Frequency [%]	12.1	6.7	0.8

Based on Table 5, for moderately dry category, 16-day SPEI identifies dry events with the highest mean and higher frequency. For severely dry category, 16-day SPI detects a high mean of dry events. For the extremely dry events, monthly SPI detect dry events with the higher means and frequency than corresponding SPEI.

At both timescales (16-day and monthly), the differences in quantifying the magnitude /degree of severity of the drought events by both SPI and SPEI could be attributed to the components they consider in their methodology. SPI only uses precipitation normalities while SPEI introduces the component of water demand (ET_{ref}) that reduces the normality of the water balance from which SPEI is computed. This significantly affects the magnitude of drought quantified, leading to the identification of more extremely dry events by SPI than SPEI (Alsafadi et al., 2020; Tirivarombo et al., 2018; Werner et al., 2015).

5.2. Agricultural drought indices

The use of vegetation index anomalies (NDVI-A & NDWI-A) as agricultural drought indices allowed for the comparison of current vegetation conditions to the long term mean conditions to monitor variations in vegetation response to climatic changes over-time (Anyamba & Tucker, 2012).

5.2.1. Temporal evolution of agricultural drought

Negative values below zero for both vegetation drought indices (NDVI-A and NDWI-A), indicate drought conditions / below normal vegetation conditions and above zero indicate non-drought conditions/ normal vegetation conditions and the degree of severity, based on the drought classification scheme in Table 2 above.

Figure 14 (a & b) illustrate line graphs of NDVI-A and NDWI-A over 2001-2020 at 16-day timescale.

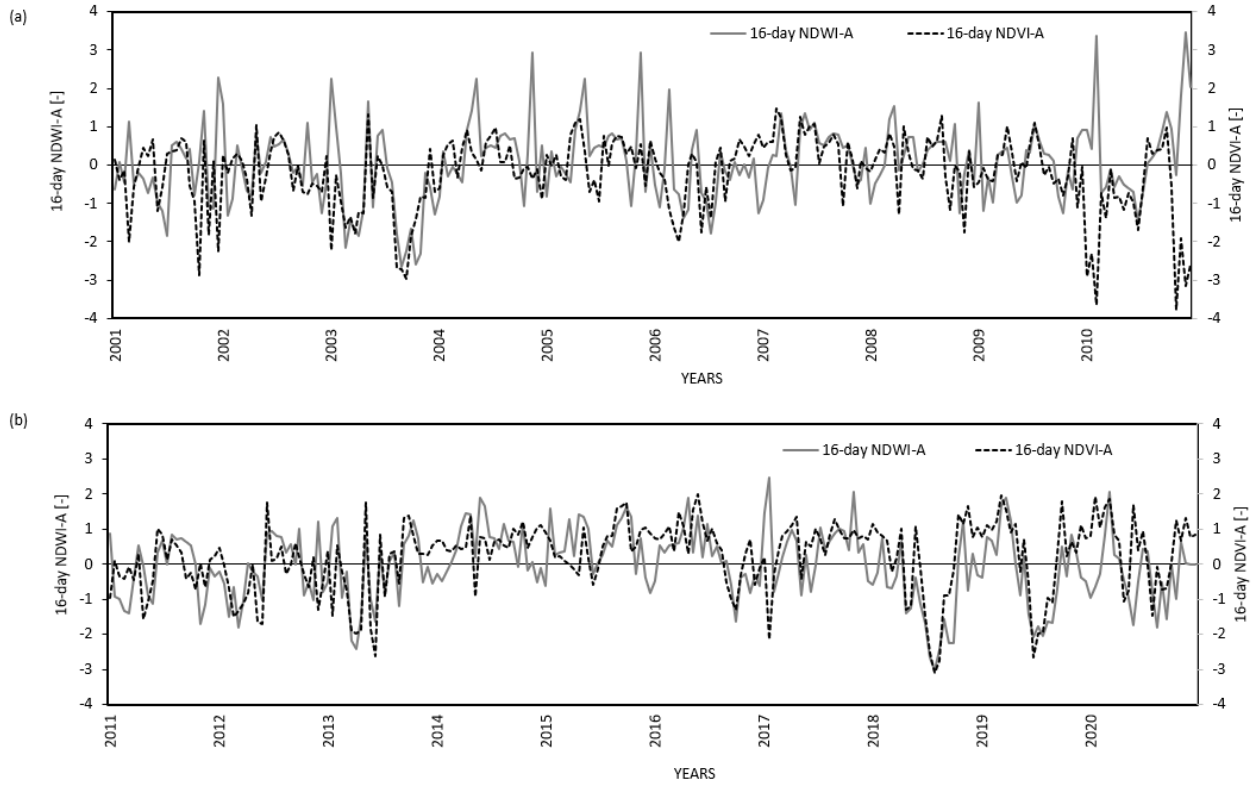

Figure 14: Temporal variations of 16-day NDVI-A timeseries and NDWI-A timeseries over 2001-2010 & 2011-2020

Based on Figure 14, the 16-day NDWI-A and NDVI-A illustrate high variations and high fluctuations in identifying non-normal conditions in majority of the years, shown by the negative peaks below zero level. A major difference is observed in 2010 where both drought indices show opposite extremes in their values at the beginning and end of the year. A further analysis of 2010 is shown in Table 4. The extreme positive peak values of NDWI-A across the years, shows its sensitivity to highly fluctuating short-term rainfall than the NDVI-A.

Correlation analysis between the 16-day NDVI-A and NDWI-A anomalies yields a significant R of 0.383, p (0.00). The research assumed the low correlation observed is affected by the extreme outliers in 2010.

Omitting 2010 records and performing a correlation analysis again, a significant correlation is yielded, R of 0.505, p (0.00).

Figure 15 (a & b) further illustrates monthly line graphs of NDVI-A and NDWI-A over the years from 2001-2020

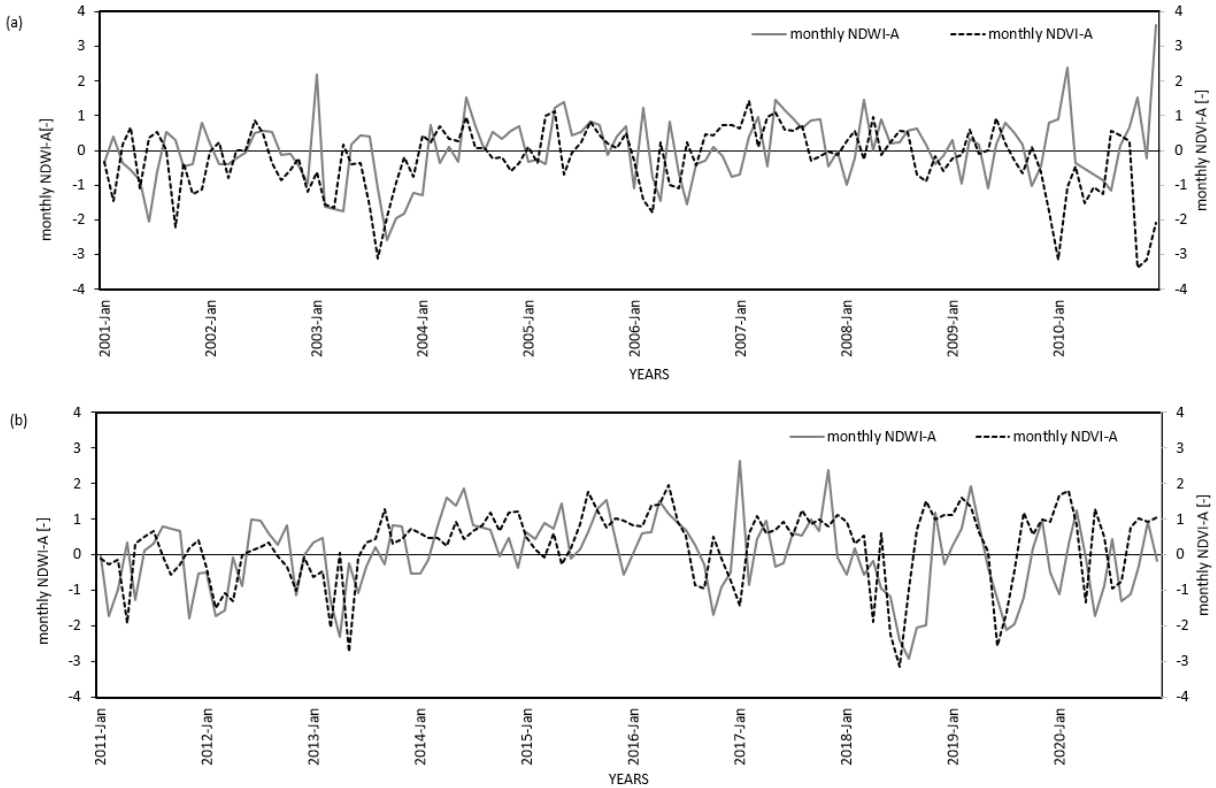

Figure 15: Temporal variations of monthly NDVI-A timeseries and NDWI-A timeseries over 2001-2010 & 2011-2020

Based on Figure 15, slight variations are observed in monthly NDVI-A and NDWI-A in their response to below normal (drought) and above normal (non-drought) conditions. Reduced fluctuations in both indices are observed especially, in the monthly NDWI-A. A time delay is clearly observed in how the monthly indices peak to drought and non-drought conditions. A non-significant low correlation (R) of 0.169, p (0.98) is yielded between the monthly vegetation index anomalies. Similar to the 16-day vegetation anomalies, the year 2010 is considered an outlier and omitted giving a new non-significant correlation, R of 0.272 p (1.00) was yielded. Further detailed analysis for the year 2010 as a case study are summarized in Table 6.

The correlation in the vegetation anomalies at both timescales shows that there exists interdependence between leaf components, that is, chlorophyll content (greenness) and leaf water content (Sellers, 1987) However, the low correlation in monthly vegetation indices indicates the differences in vegetation response to seasonal climatic patterns and the vegetative growth cycles. For instance, in winter periods it

would be expected that leaf water content would be high but no greenness since vegetation is inactive, as shown in 2010 case.

Table 6: Summary of 2010 NDVI-A and NDWI-A, and their response to monthly rainfall and monthly (ET_{ref})

2010 Monthly-timescale								
	Vegetation index anomalies		Rainfall			Etref		
	NDVI-A	NDWI-A	Total	mean	std	Total	mean	std
Jan	-3.135	0.901	32.4	65.260	34.389	6.9	47.787	35.135
Feb	-1.053	2.385	62			10.6		
Mar	-0.446	-0.375	54.5			35.6		
Apr	-1.513	-0.516	38.8			69.2		
May	-1.043	-0.697	62.5			70.1		
Jun	-1.246	-0.870	12.3			111.9		
Jul	0.573	-1.167	70.5			119.1		
Aug	0.438	0.127	229.9			67.5		
Sep	0.262	0.676	60.6			44.7		
Oct	-3.374	1.523	47.3			27.8		
Nov	-3.143	-0.221	81.2			8.6		
Dec	-2.071	3.630	43.6			5		

Table 6 illustrates further analysis of the year 2010 showing differences in how the NDVI-A and NDWI-A respond to seasonal climatic variations. The red shaded cells under vegetation index anomalies, illustrate values below (≤ -1) indicating drought events. Red shaded cells under rainfall and ET_{ref}, are the values below the thirty-three-year average monthly total rainfall and mean monthly total ET_{ref} respectively.

Based on Table 6, a contrast is observed in the response between the NDWI-A and NDVI-A response to climatic variables during the winter months (October- March). Positive NDWI-A values, associated with high leaf water content, respond positively to moderate monthly total rainfall amounts (around the mean) accompanied by low ET_{ref} values. The NDVI-A on the other hand, associated with leaf greenness (chlorophyll content) responds negatively to these climatic variables in winter period.

To better understand the role of rainfall on vegetation index anomalies, a correlation analysis is done for the whole time series (2001- 2020) between monthly total rainfall and the vegetation anomalies as illustrated in Figure 16.

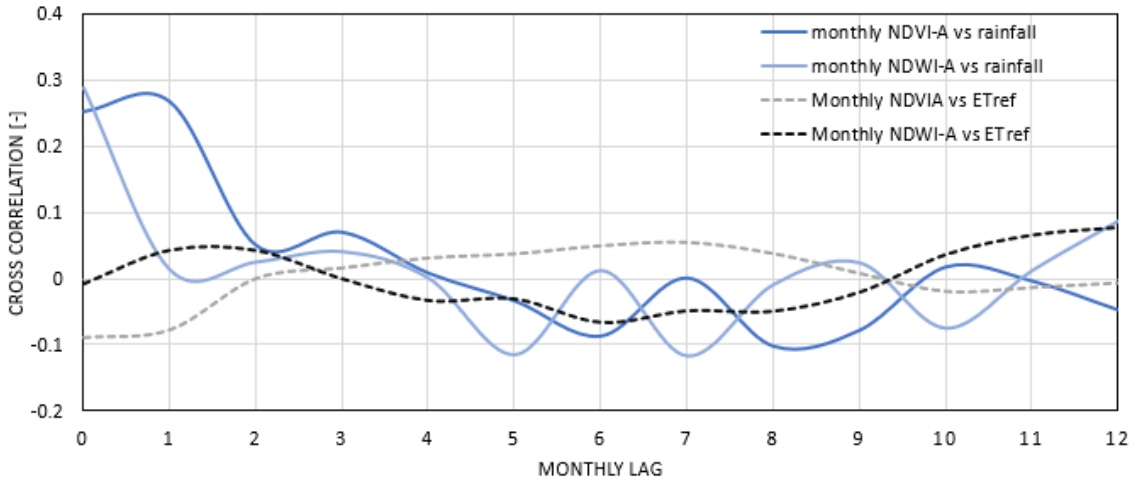

Figure 16: Time lag relationship between monthly sum rainfall and monthly sum ETref, and vegetation anomalies (NDVI-A & NDWI-A), shown by cross correlation function

In relation to rainfall, a non-significant correlation R of 0.287, p (1.00) for NDWI-A was slightly higher than a non-significant R of 0.253, p (1.00) for NDVI-A. This indicates the higher sensitivity of NDWI to rainfall than the NDVI. However, at one month lag, the NDVI-A and rainfall correlation goes up to R of 0.268 while NDWI-A goes very low to R of 0.013. These findings also support the high fluctuations in NDWI-A response at 16-days that corresponds high rainfall variability (coefficient of variation of 0.72). This supported Chakraborty & Sehgal, (2010) study that NDWI anomalies showed a better efficacy in identifying water stress in vegetation in a short-timescale of less than a month while NDVI anomalies indicated a lag relationship with moisture content in vegetation.

A negative relationship between ET_{ref} (radiation and temperature) and the monthly vegetation index anomalies is illustrated by R of -0.089 by NDVI-A and R of -0.008, by NDWI-A. The overall low correlation could be an indication of variation of solar radiation during different seasons leading to variations in ET_{ref}. However, the negative correlations for both precipitation and ET_{ref} indicates that drought conditions observed on vegetation do not only stem from these two variables.

5.2.2. Frequency of agricultural drought events and their degree of severity

To analyze the frequency of agricultural drought events and their degree of severity as identified by the vegetation index anomalies, the drought events are put in categories as classified by SPI and SPEI drought classification scheme (see Table 1).

Table 7: Summary of the degree of severity and frequency of drought events as identified by NDVI-A and NDWI-A at both 16-day and monthly timescales over the period 1988-2020 for the Twente region

Agricultural drought indices		Moderately dry	Severely dry	Extremely dry
16-day NDVI-A	Mean	**-1.268**	-1.789	-2.770
	Std dev	0.175	0.146	0.434
	Frequency [%]	6.3	4.4	3.91
16-day NDWI-A	Mean	-1.212	-1.698	-2.381
	Std dev	0.141	0.095	0.264
	Frequency [%]	7.4	4.1	3.0
Monthly NDVI-A	Mean	-1.195	-1.699	-2.704
	Std dev	0.153	0.148	0.478
	Frequency [%]	6.7	4.6	4.6
Monthly NDWI-A	Mean	-1.184	-1.750	-2.339
	Std dev	0.103	0.133	0.294
	Frequency [%]	7.5	5.8	2.9

Based on Table 7, Generally, NDVI-A identified higher means of the three categories of drought than NDWI-A. However, the drought frequencies vary between the indices. Extremely low or prolonged NDVI anomalies could be associated with instances of water stress levels that have gone beyond plant adaptive mechanisms leading to deterioration of vegetation health and a rainfall event would not lead to immediate greenness of the vegetation (Mladenova et al., 2020).

5.2.3. Trend Analysis by Mann-Kendall

Man-Kendall test was done to test whether there was a significant trend in the meteorological and vegetation drought indices at the given timescales (16-day and monthly) at 5% significance level and the results are illustrated in Table 8.

Table 8: Mann-Kendall for the meteorological and agricultural drought indices series based on 16-day and monthly timescales

Monthly Mann-Kendall Trend test (α = 0.05)				
	SPI	**SPEI**	**NDVI-A**	**NDWI-A**
16-day drought indices p-value	0.273	0.169	2.58	0.96
Monthly drought indices p-value	0.605	0.325	3.11	0.47

The Mann-Kendall (M-K) test on all the times series of the drought indices (meteorological and agricultural drought indices) from 2001-2020 show $p \geq 0.05$ that indicates that there is no significant trend in all the indices.

To test for seasonal trends, M-K test was computed based on monthly timescale for the meteorological and agricultural drought indices. The months with trends are illustrated in bold.

Table 9: Man-Kendall Trend Test on meteorological and agricultural drought indices based on monthly timescale

Monthly Mann-Kendall Trend test (α = 0.05)													
		Jan	**Feb**	**Mar**	**Apr**	**May**	**Jun**	**Jul**	**Aug**	**Sep**	**Oct**	**Nov**	**Dec**
SPI	p-value	0.792	0.877	0.676	0.168	0.768	0.780	0.901	0.792	0.306	0.678	0.889	0.722
	z-value												
SPEI	p-value	0.722	0.792	0.515	**0.036**	0.733	0.377	0.609	1.000	0.159	0.676	0.889	0.768
	z-value				**-2.092**								
NDVI-A	p-value	0.056	**0.010**	0.098	0.603	**0.048**	0.581	0.974	0.871	**0.006**	**0.001**	**0.007**	**0.005**
	z-value		**2.563**			**1.979**				**2.758**	**3.472**	**2.693**	**2.823**
NDWI-A	p-value	0.626	0.581	0.144	0.074	0.417	0.086	0.673	0.381	0.820	0.581	0.074	0.871
	z-value												

Based on Table 9, SPI shows no trend in monthly trend test, while SPEI shows a negative trend test, indicated by the negative z value in the month of April. For the agricultural drought indices, the NDWI-A shows no monthly trend while the NDVI-A shows positive trend in the drought events identified. However, the observed "no trends" could be associated with incidences of auto correlation inherent in the data series that leads to rejection of the null hypothesis (Kendall, 1948; Mann, 1945). The autocorrelations could be caused by seasonal climatic variations and vegetation growth cycles.

5.3. Soil moisture anomalies

5.3.1. Temporal evolution of soil moisture anomalies

Surface soil moisture ($\theta_{sm} - A$)/ 5 cm anomalies were computed and plotted against the root zone soil moisture anomalies (θ_{rz} -A) as shown in Figure 17. Both soil moisture anomalies illustrate a similar pattern in the response to dry and non-dry conditions over-time with an exception in 2015 where the root zone soil moisture anomalies go below surface soil moisture anomalies. The driest year identified was in July 2018 (-1.80, -1.68) corresponding to 16-day ($\theta_{sm} - A$) and (θ_{rz} -A) respectively.

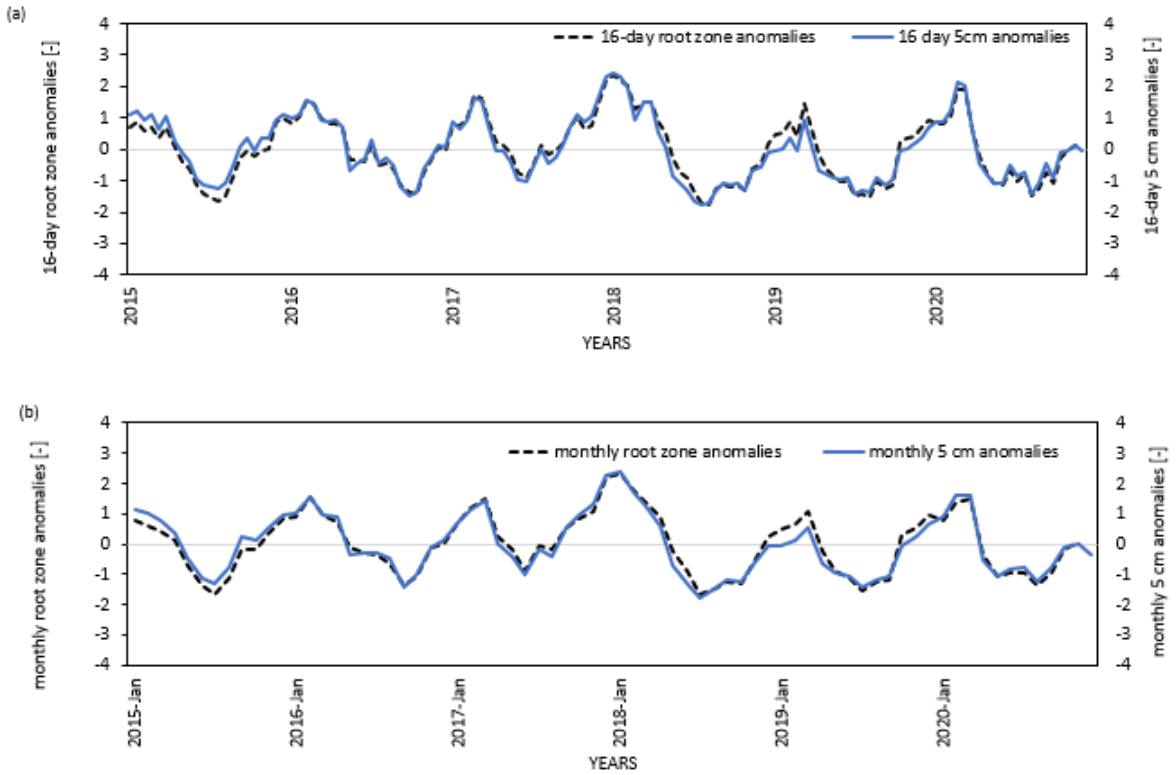

Figure 17: Temporal variations of soil moisture anomalies timeseries (a) 16-day root zone anomalies (θ_{rz} -A) and 5cm ($\theta_{sm} - A$) anomalies over 2015-2020 and (b) monthly root zone anomalies (θ_{rz} -A) and monthly 5cm ($\theta_{sm} - A$) anomalies over 2015-2020

Using 2015 as a case study, Table 10 shows the soil moisture anomalies and corresponding monthly total rainfall and monthly total (ET_{ref}). The red shaded cells under vegetation index anomalies, illustrate values below (≤ -1) indicating drought events. Red shaded cells under rainfall and ET_{ref}, are the values below the thirty-three-year average monthly total rainfall and mean monthly total ET_{ref} respectively.

Table 10: Summary of 2015 Soil moisture anomalies, and their response to monthly rainfall and monthly ETo

2015 monthly timescale								
	soil moisture anomalies		Rainfall			ETref		
	5cm anomalies	root zone anomalies	total	mean	sd	total	mean	sd
Jan	1.155	0.750	109.6	73.083	33.661	7.2	49.742	35.042
Feb	0.996	0.603	41.3			15.9		
Mar	0.801	0.437	88.2			35.3		
Apr	0.342	0.100	42.3			71.2		
May	-0.457	-0.711	40.7			81.8		
Jun	-1.131	-1.384	50.5			98.5		
Jul	-1.280	-1.666	90			101.6		
Aug	-0.783	-1.157	129.3			87.6		
Sep	0.217	-0.168	71.5			49.8		
Oct	0.120	-0.161	44.7			26.4		
Nov	0.556	0.337	129.2			12.5		
Dec	0.971	0.853	39.7			9.1		

Based on Table 10, moderate monthly total rainfall (above average) lead to positive soil moisture anomalies (5cm and root zone) due to the supply of moisture into the soil layers and reduced loss (low monthly total ET_{ref}). The root zone anomalies (θ_{rz} -A) illustrate dry events of more intensity in the summer months (Jun-Aug) than the dry events identified by $\theta_{sm} - A$)/ 5cm soil moisture anomalies. These dry events could be associated with corresponding high ET_{ref} values that lead to drying of the soil that propagates deep into the soils despite moderate rainfall. Surface anomalies ($\theta_{sm} - A$) suffer low intense dry events due to high faster replenishment of rainfall of any amount even after drying.

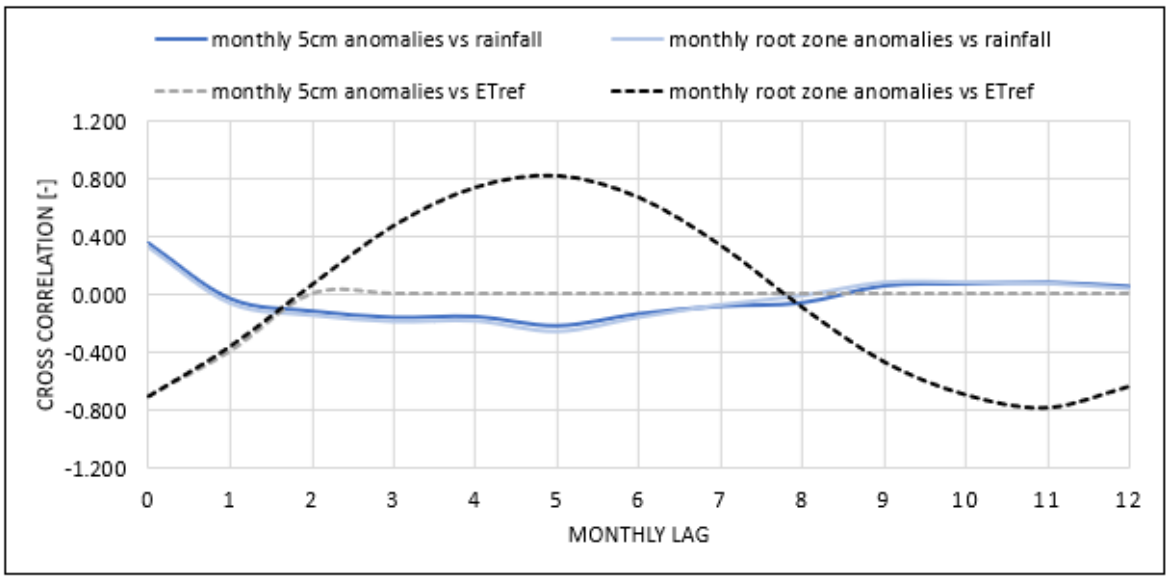

Figure 18: Time lag relationship between monthly sum rainfall and monthly sum ETref, and soil moisture anomalies (5cm and root zone), shown by cross correlation function

Based on Figure 18, the correlation analysis between soil moisture and climatic variables (precipitation and ETo) illustrates a complex relationship. Positive significant correlations are yielded between monthly precipitation and monthly 5cm anomalies ($\theta_{sm} - A$) and root zone (θ_{rz} -A), R of 0.355, p (0.00) and 0.324, p (0.00) respectively. These correlations then reduce at one month lag. Conversely, very negative correlations yield between monthly ET_{ref} and the monthly 5cm anomalies ($\theta_{sm} - A$) and root zone soil moisture anomalies (θ_{rz} -A), R of - 0.698 and - 0.693 respectively. The correlation progresses to positive values after the soil moisture anomalies are lagged backwards for two months.

These extreme correlations between soil moisture anomalies and climate variables indicate the complexity in the role of soil moisture in the climate system, that is, in land water and land energy balance (Seneviratne et al., 2010). Soil moisture influences the evapotranspiration process, leading to drying of the soils and less precipitation amounts and intense radiation, makes soil moisture a limiting factor leading to decrease in ET. This could be associated with the negative correlation values observed between soil moisture anomalies and $ET_{ref.}$

5.3.2. Frequency of drought events by soil moisture anomalies and their degree of severity

Soil moisture anomalies were used to further quantify the frequency of drought events and the degree of severity. Both 5cm anomalies ($\theta_{sm} - A$) and root zone soil moisture anomalies (θ_{rz} -A) were used. Based on Table 11, extremely dry events were not identified by the soil moisture anomalies at both timescales.

Table 11: Summary of the soil moisture anomalies based on the 16-day and monthly timescales

Soil moisture anomalies		**Moderately dry**	**Severely dry**	**Extremely dry**
16-day ($\theta_{sm} - A$)	Mean	-1.219	-1.699	-
	Std dev	0.135	0.048	
	Frequency [%]	17.6	2.3	
16-day (θ_{rz} -A)	Mean	-1.243	-1.625	-
	Std dev	0.152	0.086	
	Frequency [%]	17.6	3.8	
Monthly ($\theta_{sm} - A$)	Mean	-1.207	-1.656	-
	Std dev	0.129	0.147	
	Frequency [%]	18.1	2.8	
Monthly (θ_{rz} -A)	Mean	0.124	0.060	-
	Std dev	-1.250	-1.633	
	Frequency [%]	16.7	4.2	

Moderately dry events had a high frequency of occurrence illustrated by both soil moisture anomalies. 5cm anomalies ($\theta_{sm} - A$) illustrated a slightly higher mean of severely dry events than root zone soil moisture anomalies (θ_{rz} -A) over the six-year period at both timescales. The severe dry events identified by 5cm anomalies indicate that, despite the expected replenishment of surface soil layers by rainfall events, rapid climatic variations such as increased radiation, high temperatures and high winds reported in the region KNMI, (2020), could exacerbate the drying of the surface soils. Furthermore, the lack of extremely dry events could be associated with the region's mild and wet winter and summer seasons year round (Van Der Velde et al., 2021).

5.3.3. Relationship between meteorological &vegetation drought indices against soil moisture anomalies at 16-day timescale

To compare the temporal patterns and relationships between meteorological & vegetation drought indices against soil moisture anomalies, line graphs of SPI, SPEI, NDVI-A, NDWI-A, against 5cm soil moisture anomalies ($\theta_{sm} - A$) and root zone soil moisture anomalies (θ_{rz} -A) were plotted at 16-day timescale (Figure 19 (a) & (b))

Based on Figure 19, the 5cm anomalies ($\theta_{sm} - A$) and root zone anomalies (θ_{rz} -A) illustrate a dynamic close variation with both meteorological and vegetation indices over the period 2015-2020. The 16-day SPI and SPEI and 16-day NDVI-A and NDWI-A illustrate more frequent fluctuations and extreme peaks compared to less fluctuations in 16-day soil moisture anomalies (($\theta_{sm} - A$) and (θ_{rz} -A)). There is a clear indication of time delay / lag in how all the drought indices and soil moisture anomalies respond to drought and non-drought conditions.

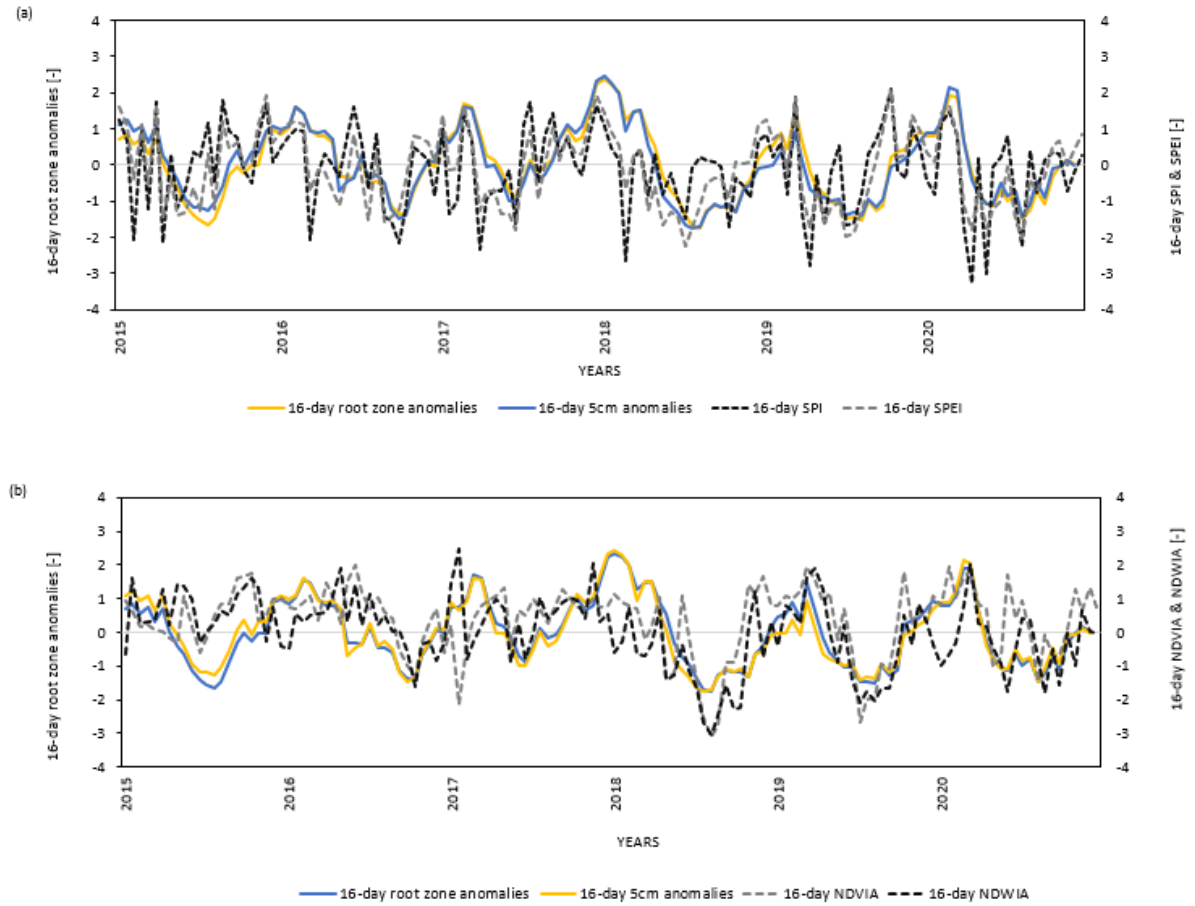

Figure 19: 16-day timeseries of meteorological drought indices (SPI & SPEI), vegetation drought indices (NDVIA & NDWIA) against 5cm anomalies ($\theta_{sm} - A$) and root zone soil moisture anomalies (θ_{rz} -A) over 2015-2020

Table 12: Pearson's correlation (R) and p-values for soil moisture anomalies and meteorological (SPI & SPEI) and vegetation drought indices (NDVI-A & NDWI-A) at 16-day timescale

16-day timescale				
	Meteorological drought indices		Vegetation drought indices	
Soil moisture anomalies	**SPI**	**SPEI**	**NDVI-A**	**NDWI-A**
5 cm anomalies	0.291	**0.624**	0.496	0.470
p-value	0.0	**0.0**	0.0	0.0
Root zone anomalies	0.336	**0.659**	0.481	0.483
p-value	0.0	**0.0**	0.0	0.0

Based on Table 12, the relationship between 5cm ($\theta_{sm} - A$) and root zone soil moisture anomalies (θ_{rz} -A) illustrate positive correlations of statistical significance with both meteorological & vegetation drought indices at 16-day timescale. However, SPEI yields the highest correlation with the soil moisture anomalies (R of 0.624, 0.659) corresponding to ($\theta_{sm} - A$) and (θ_{rz} -A) respectively. This can be explained by the

inclusion of the loss term in SPEI, that highly influences soil moisture availability as discussed under section 5.4.1. These findings are consistent with the study by S. M. Vicente-Serrano et al., (2012) who concluded that SPEI has a higher accuracy in predicting soil moisture anomalies than SPI in agricultural monitoring due to the inclusion of the moisture loss through ET_{ref} in its computation.

Root zone anomalies (θ_{rz} -A) illustrate higher correlation than 5cm anomalies ($\theta_{sm} - A$) with SPI, SPEI and NDVI-A indicating further processes that occur when precipitation falls on the surface (filtration, percolation) and subsequent loss through evapotranspiration. Conversely, the 5cm soil moisture is prone to run off or flooding depending on the antecedent soil moisture conditions reducing the correlation with meteorological indices (Seneviratne et al., 2010). A higher correlation between NDWI-A and root zone anomalies (θ_{rz} -A) indicates that NDWI (measure of leaf water content) (Gao, 1996) is highly related with the soil moisture in the lower zones of the profile where plant roots uptake their moisture.

However, some studies show a weaker correlation exists between NDVI-A /NDWI- A and the 5-cm soil layers than with deeper soil layers arguing that some plant roots have deeper roots that capture water at such depth (Gu et al., 2008). This is not the case in this research. The higher correlation of both NDVI-A and NDWI-A with surface anomalies (see Table 12), indicates that pasture (which is the common vegetation), is shallow rooted and highly influenced by surface anomalies ($\theta_{sm} - A$).

5.3.4. Relationship between meteorological &vegetation drought indices against soil moisture anomalies at monthly timescale

Further analysis of the relationship between the meteorological & vegetation drought indices against soil moisture anomalies (5cm and root zone) was done at a monthly timescale. Based on Figure 20, the monthly soil moisture anomalies illustrate a dynamic variation with both meteorological and vegetation indices with reduced fluctuations in both monthly SPI and SPEI. A visible time delay in the response to drought and non-drought conditions by all the monthly drought indices and soil moisture anomalies is observed and further explained in Figure 21.

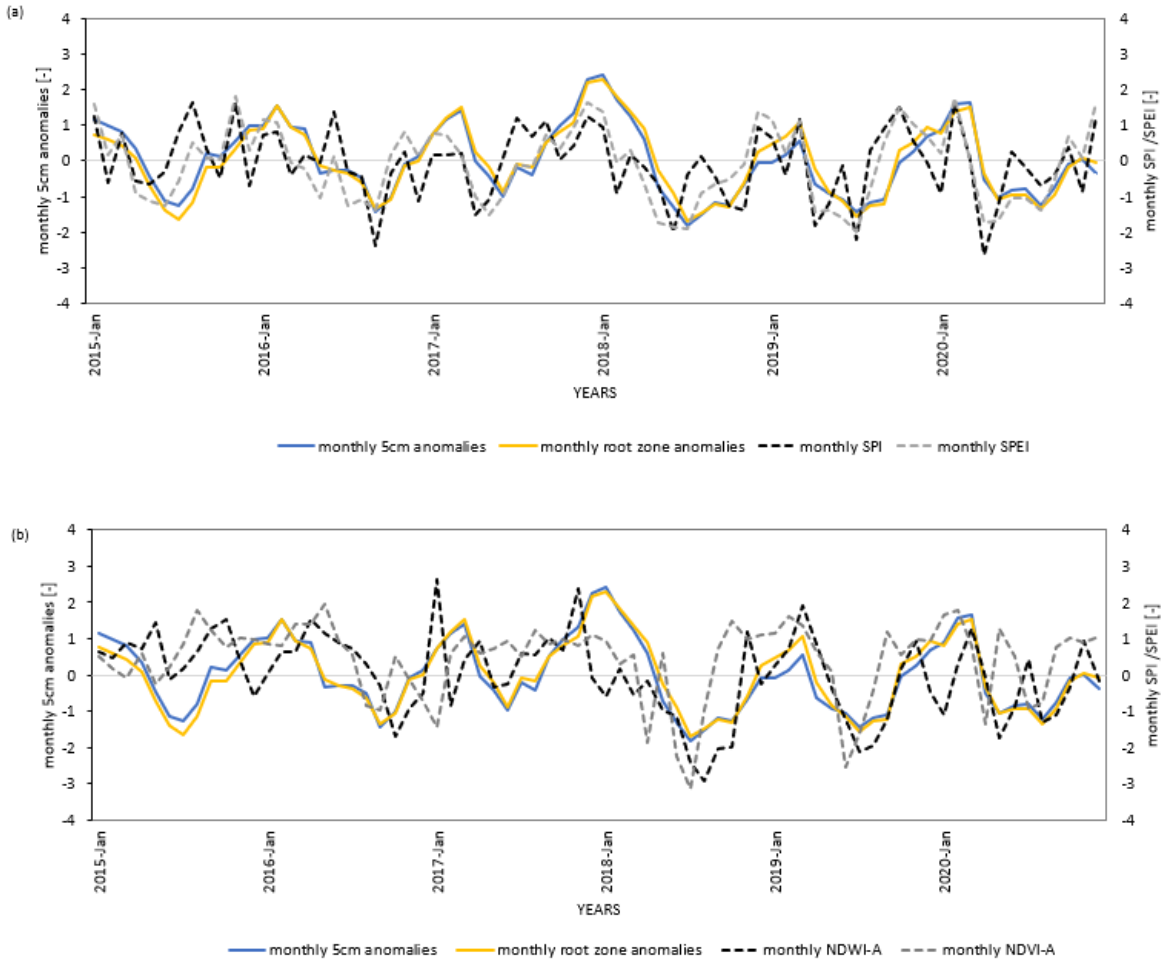

Figure 20: Graphs of monthly timeseries of meteorological drought indices (SPI & SPEI), vegetation drought indices (NDVIA & NDWIA) against 5cm soil moisture anomalies ($\theta_{sm} - A$) and root zone soil moisture anomalies (θ_{rz} -A)

For the monthly indices, SPEI yielded the highest correlation with soil moisture anomalies, followed by the NDWI-A as illustrated in Table 13. The R values were statistically significant as indicated by the p values of less than 0.05

Table 13: Pearson's correlation (R) and p-values for soil moisture anomalies and meteorological (SPI & SPEI) and vegetation drought indices (NDVI-A & NDWI-A) at monthly timescale

	monthly timescale			
	Meteorological drought indices		**Vegetation drought indices**	
Soil moisture anomalies	**SPI**	**SPEI**	**NDVI-A**	**NDWI-A**
5 cm anomalies	0.343	**0.660**	0.382	0.490
p-value	0.0	**0.0**	0.0	0.0
Root zone anomalies	0.381	**0.679**	0.379	0.478
p-value	0.0	**0.0**	0.0	0.0

To investigate lagged responses of the meteorological (SPI & SPEI), vegetation drought indices (NDVI-A & NDWI-A) on soil moisture anomalies, graphs of monthly time lag were plotted.

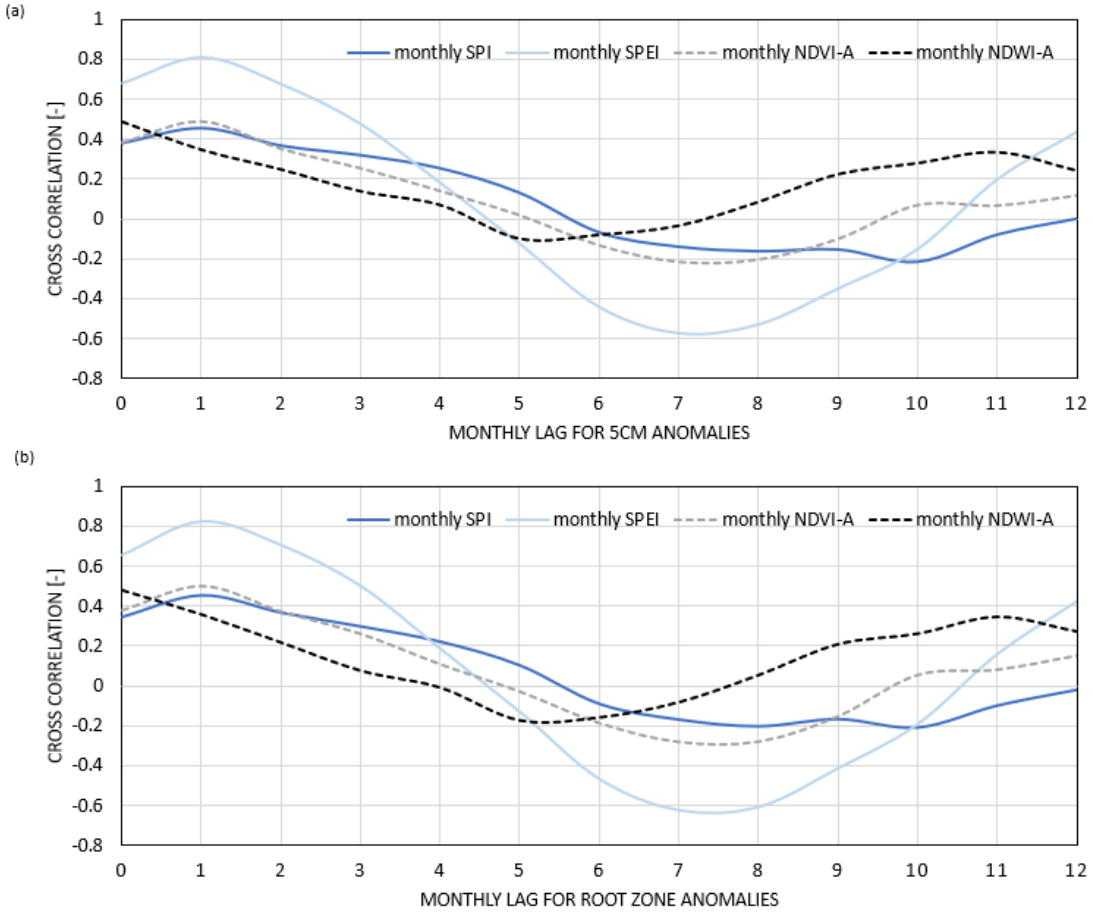

Figure 21: Graphs of time lag relationship between monthly meteorological drought indices (SPI & SPEI), vegetation drought indices, and (a) 5cm soil moisture anomalies, (b) root zone soil moisture anomalies, shown by cross correlation function

Based on Figure 21, when soil moisture anomalies were lagged backwards, the SPEI illustrates its superiority over all indices in the relationship with soil moisture anomalies, shown by the highest correlation (0.808, 0.828) corresponding to ($\theta_{sm} - A$) and (θ_{rz} -A) a lag of one month. The NDWI-A shows a high correlation at zero-time lag with R of (0.490, 0.478) corresponding to ($\theta_{sm} - A$) and (θ_{rz} -A) and reduces its correlation at the one-month lag. The exceptional results of NDWI-A indicate a high relationship exists between soil moisture content and leaf water content in vegetation (Chen et al., 2005; Cheng, 2007). Low correlation between NDVI-A and soil moisture anomalies could be attributed to seasonal patterns of high radiation (summer) and low radiation (winter) that influence heavily the "greenness" of vegetation in combination to moisture availability.

5.4. 2018 as an exceptional drought year

Based on all the indices, 2018 was identified as a drought year which coincided with KNMI reports of the highest precipitation deficits recorded (KNMI, 2020). Table 14 indicates the drought events as identified by monthly soil moisture anomalies (($\theta_{sm} - A$) and (θ_{rz} -A)), meteorological drought indices (SPI and SPEI) and agricultural drought indices (NDVI-A and NDWI-A). The red shaded cells under vegetation index anomalies, illustrate values below (≤ -1) indicating drought events.

Table 14: Summary of the 2018 drought events identified by meteorological and agricultural drought indices at monthly timescale

2018 Monthly Timescale						
	soil moisture anomalies		meteorological drought indices		agricultural drought indices	
	5cm anomalies	root zone anomalies	SPI	SPEI	NDVI-A	NDWI-A
Jan	2.40	2.30	0.949	1.374	2.304	-0.573
Feb	1.74	1.81	-0.918	-0.027	1.812	0.184
Mar	1.25	1.36	0.155	0.309	1.364	-0.560
Apr	0.59	0.90	-0.179	-0.647	0.900	-0.165
May	-0.73	-0.25	-0.672	-1.736	-0.245	-0.952
Jun	-1.29	-0.90	-1.982	-1.856	-0.900	-1.159
Jul	-1.80	-1.68	-0.399	-1.901	-1.685	-2.408
Aug	-1.51	-1.49	0.128	-0.895	-1.488	-2.904
Sep	-1.19	-1.22	-0.420	-0.649	-1.225	-2.034
Oct	-1.26	-1.30	-1.258	-0.543	-1.295	-1.986
Nov	-0.67	-0.59	-1.383	-0.092	-0.589	1.199
Dec	-0.06	0.25	0.954	1.395	0.246	-0.268

Based on Table 14, the vegetation index anomalies (agricultural drought indices) correspond to the soil moisture anomalies, especially in the summer months (June- September). The SPEI identifies a higher number of events than SPI during these months. This is a clear indication that the agricultural droughts of this year were not affected by limited moisture but possibly other factors such as intense radiation, and increased temperatures. The extreme dry events (≤ 2.0) observed in NDWI-A could be attributed to high evaporative water demand leading to increased water stress in vegetation. van Hateren et al. (2021) pointed identified droughts that were energy limited in 2003 and 2005 in some parts of Europe.

5.5. Assumptions / Limitations of the study

The SPI and SPEI values are derived from probability distribution functions that assume that the PDFs provide valid fitting of the meteorological variables. Gamma and log-logistic PDFs were tested against the empirical distributions derived from the meteorological variables (precipitation and water balance).

This research assumed the role of seasonal patterns in how meteorological and agricultural droughts indices would respond to different seasons in a year and the associated seasonal climatic variability. This was tested using the M-K Test trend analysis on monthly drought indices to capture any trends over-time.

SPI has been suggested to have incidences of skewed SPI values when using short term time scales of weeks (Edwards & Mckee, 1997; Wu et al., 2007). In this research, to eliminate the skewed SPI, low precipitation values were omitted recommended by Wu et al., (2007) in the application of SPI in arid areas and dry seasons. Soil moisture variability, vertically and horizontally, caused by factors such as different soil types was not considered in the generation of root zone soil moisture. Insufficient remote sensing data (2001-2020) led to computation of meteorological indices that ran for the same period 2001-2020, however, based on thirty-three-year rainfall and ET_{ref} climatology the M-K test was used to test the significance of the trends in droughts identified by all the drought indices (SPI, SPEI, NDVI-A &NDWI-A) for the whole period (2001-2020). To account for seasonal changes, monthly trend tests using the M-K test were done. Insufficient soil moisture data (2015-2020) led to the comparison of the drought indices with soil moisture anomalies foe the period (2015-2020). The correlation results were tested for significance using the p test values at 5% significance level.

6. CONCLUSION AND RECOMMENDATIONS

6.1. Summary and Conclusion

In this research, both meteorological and vegetation drought indices were assessed on their capability to detect short-term droughts observed in meteorological and agricultural droughts. The findings of this research indicated that in the detection of meteorological droughts, SPI quantified severe (≤ -1.5) to extremely (≤ -2.0) dry events shown by higher mean values than SPEI at both timescales. Conversely, SPEI quantified droughts of moderate (≤-1) dryness of high frequency indicating the consideration of the demand component in drought monitoring. For vegetation drought indices, the 16-day NDVI-A illustrated high means of moderate, severely dry, and extremely dry events with a variation in frequency. Monthly NDWI-A showed slightly high mean for severely dry events. These illustrated the differences in how vegetation components (leaf water content, chlorophyll content) respond to drought and non-drought conditions at various timescales.

A higher significant correlation, R of 0.505, p (0.0) was observed between 16-days NDWI-A and NDVI-A in comparison to a non-significant correlation R of 0.272, p (0.0) between monthly NDWI-A and NDVI-A. This indicated the short-term interdependence between the leaf components (chlorophyll content and leaf water content). High fluctuations in 16-day NDWI-A which reduced in monthly NDWI-A illustrated the influence of short-term high moisture variability on the leaf water content.

Further findings of the relationship between vegetation index anomalies and rainfall showed that the both monthly vegetation indices showed low correlations of non-significance, R of 0.287, p (1.0) and (R of 0.253, p (1.0) corresponding to monthly NDWI-A and NDVI-A respectively. When rainfall was lagged backwards for a month, the NDWI-A correlation reduced whereas the correlation between NDVI-A and the monthly total rainfall increased. A negative relationship occurred when the vegetation drought indices were compared to ET_{ref}, illustrated by NDWI-A negative correlation R of -0.089 and NDVI-A R of -0.008. This could be due to the variation of solar radiation during different seasons. These low correlations between the vegetation drought indices and climate variables indicated that drought observed in vegetation is not entirely depended on climatic variability.

The comparison of the droughts identified by both surface soil /5cm anomalies ($\theta_{sm} - A$) and root zone moisture anomalies (θ_{rz} -A), indicated that both anomalies captured high moderately dry events. However, 5cm anomalies ($\theta_{sm} - A$) identified high mean of severely dry events than (θ_{rz} -A) indicating the top layers to be prone to rapid climatic variations such as high temperatures, high winds imposing a strong control on the available soil moisture content. The comparison between monthly soil moisture

anomalies and rainfall yielded significant positive correlations (R of 0.355, p (0.0) and 0.324, p (0.0)) with corresponding ($\theta_{sm} - A$) and (θ_{rz} -A). However, when the monthly soil moisture anomalies were compared with monthly ET_{ref}, extremely negative correlations were observed with R values of - 0.698 and - 0.693 for ($\theta_{sm} - A$) and (θ_{rz} -A), respectively. These differences in the relationship between climatic variables and soil moisture anomalies display the complexities of the role of soil moisture in the climate feedbacks.

SPEI yielded significantly the highest correlation with the soil moisture anomalies R of > 0.6, p (0.0) at 16-day timescale and monthly timescale among all the drought indices used in the research. This high correlation can be explained by the inclusion of the loss term (ET_{ref}) in SPEI, that highly influences soil moisture availability. The NDWI-A yielded a significant higher correlation than NDVI-A with soil moisture anomalies R of >0.4, p (0.0) without a time delay /lag. When soil moisture was lagged backwards, the NDVI-A, increased the correlation while the NDWI-A correlation reduced. This illustrated the quicker response of leaf water content to soil moisture anomalies than chlorophyll content "greenness".

In the trend analysis with Mann -Kendall (M-K) test on monthly time series of all drought indices, only a few months showed trends. The SPEI indicated a trend in April an indication of drying springs associated with higher temperatures, high radiation and lower rainfall as depicted earlier in the long-term average ET_{ref}. The NDVIA showed trends in the months of (Feb, May, Sep, Oct, Nov & Dec) an indication of varying response in vegetation to the climatic variability overtime.

For the case of 2018, the SPEI showed a higher number of events than SPI during the summer months as observed by soil moisture anomalies. Both vegetation indices (NDVI-A and NDWI-A) responded to these soil moisture anomalies with NDWI-A showing droughts of extremely dry events (≤ 2.0). These responses by SPEI and NDWI-A indicated the contribution of high evaporative water demand to increased water stress in vegetation.

The research concluded that SPEI and NDWI-A were the preferred drought indices for estimating agricultural droughts based on their high correlation with soil moisture anomalies in Twente region. The combination of meteorological drought indices and remotely sensed vegetation indices provided a holistic approach in estimating agricultural droughts observed by soil moisture anomalies leading to reliable conclusions.

6.2. Recommendations

The good performance of SPEI in its relationship with soil moisture anomalies could be a potential alternative drought indicator by KNMI over the commonly used drought indicator, "het potentiele neerslagtekort".

The study recommended further studies on the potential of using soil moisture anomalies to monitor hydrological droughts in the region, important for ground water investigations.

The low variations in how 5 cm anomalies ($\theta_{sm} - A$) and root zone soil moisture anomalies (θ_{rz} -A) responded to the meteorological and vegetation drought indices recommended the potential use remote sensed surface soil moisture for agricultural drought monitoring for the Twente region.

LIST OF REFERENCES

Abramowitz, M., & Irene, S. (1970). *Handbook of Mathematical Functions With Formulas, Graphs, and Matheamtical Tables* (9th ed.). U.S.Government Printing Office.

Abrams, M. D., Ruffner, C., & Morgan, T. A. (1998). Tree-Ring Responses to Drought Across Species and Contrasting Sites in the Ridge and Valley of Central Pennsylvania. *Forest Science*. https://www.researchgate.net/publication/233557463_Note_Tree-Ring_Responses_to_Drought_Across_Species_and_Contrasting_Sites_in_the_Ridge_and_Valley_of_Central_Pennsylvania

Akinremi, O. ., McGinn, S. M., & Barr, A. G. (1996). (PDF) Evaluation of the Palmer Drought Index on the Canadian Prairies. *Journal of Climate*, *9*.

Allen, G. R., Pereira, S. L., Raes, D., & Smith, M. (1998). FAO Irrigation and Drainage Paper Crop by. *Irrigation and Drainage*, *300*(56), 300. https://doi.org/10.1016/j.eja.2010.12.001

Alsafadi, K., Mohammed, S. A., Ayugi, B., Sharaf, M., & Harsányi, E. (2020). Spatial–Temporal Evolution of Drought Characteristics Over Hungary Between 1961 and 2010. *Pure and Applied Geophysics*, *177*(8), 3961–3978. https://doi.org/10.1007/s00024-020-02449-5

Anderson, L. O., Malhi, Y., Aragão, L. E. O. C., Ladle, R., Arai, E., Barbier, N., & Phillips, O. (2010). Remote sensing detection of droughts in Amazonian forest canopies. *New Phytologist*, *187*(3), 733–750. https://doi.org/10.1111/j.1469-8137.2010.03355.x

Anyamba, A., & Tucker, C. J. (2012). *Historical Perspectives on AVHRR NDVI and Vegetation Drought Monitoring*. NASA Publications. http://digitalcommons.unl.edu/nasapub/217

Ariyanto, D. P., Aziz, A., Komariah, Sumani, & Abara, M. (2020). Comparing the accuracy of estimating soil moisture using the standardized precipitation Index (SPI) and the standardized precipitation evapotranspiration index (SPEI). *Sains Tanah*, *17*(1), 23–29. https://doi.org/10.20961/stjssa.v17i1.41396

Brázdil, R., Kiss, A., Luterbache, J., Nash, D. J., & Řezníčková, L. (2018). Documentary data and the study of past droughts: A global state of the art. *Climate of the Past*, *14*(12), 1915–1960. https://doi.org/10.5194/cp-14-1915-2018

Brown, J. F., Wardlow, B. D., Tadesse, T., Hayes, M. J., & Reed, B. C. (2008). The Vegetation Drought Response Index (VegDRI): A new integrated approach for monitoring drought stress in vegetation. *GIScience and Remote Sensing*, *45*(1), 16–46. https://doi.org/10.2747/1548-1603.45.1.16

Buitink, J., Swank, A. M., van der Ploeg, M., Smith, N. E., Benninga, H.-J. F., van der Bolt, F., Carranza, C. D. U., Koren, G., van der Velde, R., & Teuling, A. J. (2020). Anatomy of the 2018 agricultural drought in The Netherlands using in situ soil moisture and satellite vegetation indices satellite imagery. *Hydrology and Earth System Sciences*, *August*, 1–17.

Byun, H. R., & Wilhite, D. A. (1999). Objective quantification of drought severity and duration. *Journal of Climate*, *12*(9), 2747–2756. https://doi.org/10.1175/1520-0442(1999)012<2747:OQODSA>2.0.CO;2

Carranza, C., Nolet, C., Pezij, M., & van der Ploeg, M. (2021). Root zone soil moisture estimation with Random Forest. *Journal of Hydrology*, *593*(October 2020), 125840. https://doi.org/10.1016/j.jhydrol.2020.125840

Carter, G. A. (1994). Ratios of leaf reflectances in narrow wavebands as indicators of plant stress. *International Journal of Remote Sensing*, *15*(3), 517–520. https://doi.org/10.1080/01431169408954109

Chakraborty, A., & Sehgal, V. K. (2010). *Assessment of Agricultural Drought Using MODIS Derived Normalized Difference Water Index*. *10*(May 2014), 28–36.

Chakravarti, I. ., Laha, R. G., & Roy, J. (1967). *Handbook of Methods of Applied Statistics*. John Wiley & Sons, Ltd.

Chen, D., Huang, J., & Jackson, T. J. (2005). Vegetation water content estimation for corn and soybeans using spectral indices derived from MODIS near- and short-wave infrared bands. *Remote Sensing of Environment*, *98*(2–3), 225–236. https://doi.org/10.1016/j.rse.2005.07.008

Cheng, Y.B. (2007). Relationships between Moderate Resolution Imaging Spectroradiometer water indexes and tower flux data in an old growth conifer forest. *Journal of Applied Remote Sensing*, *1*(1), 013513. https://doi.org/10.1117/1.2747223

Dai, A. (2013). Increasing drought under global warming in observations and models. In *Nature Climate Change* (Vol. 3, Issue 1). Nature Publishing Group. https://doi.org/10.1038/nclimate1633

De Oliveira, J. C., & Epiphanio, J. C. N. (2012). Noise reduction in MODIS NDVI time series data based on spatial-temporal analysis. *International Geoscience and Remote Sensing Symposium (IGARSS)*, *January 2012*, 2372–2375. https://doi.org/10.1109/IGARSS.2012.6350807

Dente, L., Vekerdy, Z., Su, Z., & Ucer, M. (2011). *Twente soil moisture and soil temperature monitoring network*. *October*, 19. http://www.itc.nl/library/papers_2011/scie/dente_twe.pdf

Di, L., Rundquist, D. C., & Han, L. (1994). Modelling relationships between ndvi and precipitation during vegetative growth cycles. *International Journal of Remote Sensing*, *15*(10), 2121–2136. https://doi.org/10.1080/01431169408954231

Didan, K., Munoz, A. B., Solano, R., & Huete, A. (2015). *MODIS Vegetation Index User 's Guide (Collection 6)* (Vol. 2015, Issue May).

Edwards, D. C., & Mckee, T. B. (1997). Characteristics of 20th Century Drought in the United States at Multiple Time scales. In *Climatology Report* (Issue 634). http://weather.uwyo.edu/upperair/sounding.html

Feyen, L., & Dankers, R. (2009). Impact of global warming on streamflow drought in Europe. *Journal of Geophysical Research*, *114*(D17), D17116. https://doi.org/10.1029/2008JD011438

Flach, B., & Phillips, S. (2018). *Netherlands: The Diverse Effects of the Drought*. https://www.fas.usda.gov/data/netherlands-diverse-effects-drought

Fu, Z., Ciais, P., Bastos, A., Stoy, P. C., Yang, H., Green, J. K., Wang, B., Yu, K., Huang, Y., Knohl, A., Šigut, L., Gharun, M., Cuntz, M., Arriga, N., Roland, M., Peichl, M., Migliavacca, M., Cremonese, E., Varlagin, A., … Koebsch, F. (2020). Sensitivity of gross primary productivity to climatic drivers during the summer drought of 2018 in Europe: Sensitivity of GPP to climate drivers. *Philosophical Transactions of the Royal Society B: Biological Sciences*, *375*(1810). https://doi.org/10.1098/rstb.2019.0747

Gallo, K. P., Daughtry, C. S. T., & Bauer, M. E. (1985). Spectral Estimation of Absorbed Photosynthetically Active Radiation in Corn Canopies*. *Remote Sensing of Environment*, *17*, 221–232.

Gao, B. C. (1996). NDWI - A normalized difference water index for remote sensing of vegetation liquid water from space. *Remote Sensing of Environment*, *58*(3), 257–266. https://doi.org/10.1016/S0034-4257(96)00067-3

Genidy, M. El. (2020). Three Parameters Estimation of Log-Logistic Distribution Using Algorithm of Three Parameters Estimation of Log-Logistic Distribution Using Algorithm of Percentile Roots. *The 54th Annual Conference on Statistics, Computer Science and Operation Research 9-11 Dec, 2019*, *December 2019*.

Greenland, S., Senn, S. J., Rothman, K. J., Carlin, J. B., Poole, C., Goodman, S. N., & Altman, D. G. (2016). Statistical tests, P values, confidence intervals, and power: a guide to misinterpretations. *European Journal of Epidemiology*, *31*(4), 337–350. https://doi.org/10.1007/s10654-016-0149-3

Gu, Y., Brown, J. F., Verdin, J. P., & Wardlow, B. (2007). A five-year analysis of MODIS NDVI and NDWI for grassland drought assessment over the central Great Plains of the United States. *Geophysical Research Letters*, *34*(6), 1–6. https://doi.org/10.1029/2006GL029127

Gu, Y., Hunt, E., Wardlow, B., Basara, J. B., Brown, J. F., & Verdin, J. P. (2008). Evaluation of MODIS NDVI and NDWI for vegetation drought monitoring using Oklahoma Mesonet soil moisture data. *Geophysical Research Letters*, *35*(22), 1–5. https://doi.org/10.1029/2008GL035772

Gutman, G. G. (1990). Towards Monitoring Droughts from Space. *Journal of Climate*, *3*(2), 282–295. https://doi.org/10.1175/1520-0442(1990)003<0282:tmdfs>2.0.co;2

Guttman, N. B. (1998). Comparing the palmer drought index and the standardized precipitation index. *Journal of the American Water Resources Association*, *34*(1), 113–121. https://doi.org/10.1111/j.1752-1688.1998.tb05964.x

Gwak, Y. S., Kim, Y. T., Won, C. H., & Kim, S. H. (2017). The relationships between drought indices (SPI, API) and in-situ soil moisture in forested hillslopes. *WIT Transactions on Ecology and the Environment*, *220*, 217–224. https://doi.org/10.2495/WRM170211

Hendriks, D. M. D., Kuijper, M. J. M., & van Ek, R. (2014). Groundwater impact on environmental flow needs of streams in sandy catchments in the Netherlands. In *Hydrological Sciences Journal* (Vol. 59, Issues 3–4, pp. 562–577). https://doi.org/10.1080/02626667.2014.892601

Hiemstra, P., & Sluiter, R. (2011). Interpolation of Makkink Evaporation in the Netherlands. In *De Bilt, 2011 | Technical report; TR-327*. http://www.numbertheory.nl/files/report_evap.pdf

Holzman, M. E., Rivas, R., & Piccolo, M. C. (2014). Estimating soil moisture and the relationship with crop yield using surface temperature and vegetation index. *International Journal of Applied Earth Observation and Geoinformation*, *28*(1), 181–192. https://doi.org/10.1016/j.jag.2013.12.006

Huete, A. R., Liu, H. Q., Batchily, K., & Van Leeuwen, W. (1997). A comparison of vegetation indices over a global set of TM images for EOS-MODIS. *Remote Sensing of Environment*, *59*(3), 440–451.

https://doi.org/10.1016/S0034-4257(96)00112-5
Hui-Mean, F., Yusop, Z., & Yusof, F. (2018). Drought analysis and water resource availability using standardised precipitation evapotranspiration index. *Atmospheric Research*, *201*(August 2017), 102–115. https://doi.org/10.1016/j.atmosres.2017.10.014
Hussain, M., & Mahmud, I. (2019). pyMannKendall: a python package for non parametric Mann Kendall family of trend tests. *Journal of Open Source Software*, *4*(39), 1556. https://doi.org/10.21105/joss.01556
Illowsky, B., & Dean, S. (2021). *Testing the Significance of the Correlation Coefficient*. https://stats.libretexts.org/Bookshelves/Introductory_Statistics/Book%3A_Introductory_Statistics_(OpenStax)/12%3A_Linear_Regression_and_Correlation/12.05%3A_Testing_the_Significance_of_the_Correlation_Coefficient
Ji, L., & Peters, A. J. (2003). Assessing vegetation response to drought in the northern Great Plains using vegetation and drought indices. *Remote Sensing of Environment*, *87*(1), 85–98. https://doi.org/10.1016/S0034-4257(03)00174-3
Karmeshu, N. (2012). *Trend Detection in Annual Temperature & Precipitation using the Mann Kendall Test-A Case Study to Assess Climate Change on Select States in the Northeastern United States* [University of Pennsylvania ScholarlyCommons]. http://repository.upenn.edu/mes_capstoneshttp://repository.upenn.edu/mes_capstones/47http://repository.upenn.edu/mes_capstones/47
Kendall, M. (1948). *Rank correlation methods*. https://psycnet.apa.org/record/1948-15040-000
Keyantash, J., & Dracup, J. (2002). An Evaluation of a Drought. *American Meteorological Society*, *August*, 1167–1180.
KNMI. (2020). *More frequent drought in the interior*. KNMI - Vaker Droogte in Het Binnenland. https://www.knmi.nl/over-het-knmi/nieuws/vaker-droogte-in-het-binnenland
Kross, A. (2005). *Evaluating the applicability of MODIS data for phenological monitoring in The Netherlands* (Issue June). https://doi.org/10.13140/RG.2.1.4631.5125
Li, R., Tsunekawa, A., & Tsubo, M. (2014). Index-based assessment of agricultural drought in a semi-arid region of Inner Mongolia, China. *Journal of Arid Land*, *6*(1), 3–15. https://doi.org/10.1007/s40333-013-0193-8
Lindsey, R., & Herring, D. (1990). The moderate resolution imaging spectrometer (MODIS). In *28th Aerospace Sciences Meeting, 1990*. https://doi.org/10.2514/6.1990-166
Lloyd-Hughes, B., & Saunders, M. A. (2002). A drought climatology for Europe. *International Journal of Climatology*, *22*(13), 1571–1592. https://doi.org/10.1002/joc.846
Mann, H. B. (1945). Non-Parametric Test Against Trend. *Econometrica*, *13*(3), 245–259. http://www.economist.com/node/18330371?story%7B_%7Did=18330371
McCarthy, J. J., Canziani, O. F., Leary, N. A., Dokken, D. J., & White, K. S. (2001). *Climate Change 2001 Impacts, Adaptation, and Vulnerability*. Cambridge University Press. http://www.cambridge.org
Mckee, T. B., Doesken, N. J., & Kleist, J. (1993). The relationship of drought frequency and duratin to time scales. *Eighth Conference on Applied Climatology*, 17–22. https://climate.colostate.edu/pdfs/relationshipofdroughtfrequency.pdf
Mehr, A. D., & Babak, V. (2019). Identification of the trends associated with the SPI and SPEI indices across Ankara, Turkey. *Theoretical and Applied Climatology*, *139*(3–4), 1531–1542. https://doi.org/10.1007/s00704-019-03071-9
Mennis, J. (2001). Exploring relationships between ENSO and vegetation vigour in the South-east USA using AVHRR data. *International Journal of Remote Sensing*, *22*(16), 3077–3092. https://doi.org/10.1080/01431160152558251
Mishra, A. K., & Singh, V. P. (2010). A review of drought concepts. *Journal of Hydrology*, *391*(1–2), 202–216. https://doi.org/10.1016/j.jhydrol.2010.07.012
Mladenova, I. E., Bolten, J. D., Crow, W., Sazib, N., & Reynolds, C. (2020). Agricultural Drought Monitoring via the Assimilation of SMAP Soil Moisture Retrievals Into a Global Soil Water Balance Model. *Frontiers in Big Data*, *3*. https://doi.org/10.3389/fdata.2020.00010
Nanzad, L., Zhang, J., Tuvdendorj, B., Nabil, M., Zhang, S., & Bai, Y. (2019). NDVI anomaly for drought monitoring and its correlation with climate factors over Mongolia from 2000 to 2016. *Journal of Arid Environments*, *164*, 69–77. https://doi.org/10.1016/j.jaridenv.2019.01.019
Naresh, K. M., Murthy, C. S., Sesha Sai, M. V. R., & Roy, R. S. (2009). On the Use of Standardized Precipitation Index (SPI) for drought intensity assessment. *Meteorological Applications*, *16*, 381–389. https://doi.org/10.1002/met.136
Nicholson, S. E., & Farrar, T. J. (1994). The influence of soil type on the relationships between NDVI,

rainfall, and soil moisture in semiarid Botswana. I. NDVI response to rainfall. *Remote Sensing of Environment*, *50*(2), 107–120. https://doi.org/10.1016/0034-4257(94)90038-8
Oliveira-Júnior, J. F., De Gois, G., De Bodas Terassi, P. M., Da Silva Junior, C. A., Blanco, C. J. C., Sobral, B. S., & Gasparini, K. A. C. (2018). Drought severity based on the SPI index and its relation to the ENSO and PDO climatic variability modes in the regions North and Northwest of the State of Rio de Janeiro - Brazil. *Atmospheric Research*, *212*(May), 91–105. https://doi.org/10.1016/j.atmosres.2018.04.022
Osman, M., Zaitchik, B. F., Badr, H. S., Christian, J. I., Tadesse, T., Otkin, J. A., & Anderson, M. C. (2021). Flash drought onset over the contiguous United States: Sensitivity of inventories and trends to quantitative definitions. *Hydrology and Earth System Sciences*, *25*(2), 565–581. https://doi.org/10.5194/hess-25-565-2021
Pachauri, R. K., & Meyer, L. (2014). Climate Change 2014. In *Synthesis Report. Contribution of Working Groups I, II and III to the Fifth Assessment Report of the Intergovernmental Panel on Climate Change*.
Palmer, W. C. (1965). *Meteorological Drought*.
Paruelo, J. M., & Lauenroth, W. K. (1995). Regional patterns of normalized difference vegetation index in North American shrublands and grasslands. *Ecology*, *76*(6), 1888–1898. https://doi.org/10.2307/1940721
Pei, Z., Fang, S., Wang, L., & Yang, W. (2020). Comparative analysis of drought indicated by the SPI and SPEI at various timescales in inner Mongolia, China. *Water (Switzerland)*, *12*(7). https://doi.org/10.3390/w12071925
Peña-Gallardo, M., Martín Vicente-Serrano, S., Domínguez-Castro, F., & Beguería, S. (2019). The impact of drought on the productivity of two rainfed crops in Spain. *Natural Hazards and Earth System Sciences*, *19*(6), 1215–1234. https://doi.org/10.5194/nhess-19-1215-2019
Peng, L., Li, D., & Sheffield, J. (2018). Drivers of Variability in Atmospheric Evaporative Demand: Multiscale Spectral Analysis Based on Observations and Physically Based Modeling. *Water Resources Research*, *54*(5), 3510–3529. https://doi.org/10.1029/2017WR022104
Peñuelas, J., Gamon, J. A., Fredeen, A. L., Merino, J., & Field, C. B. (1994). Reflectance indices associated with physiological changes in nitrogen- and water-limited sunflower leaves. *Remote Sensing of Environment*, *48*(2), 135–146. https://doi.org/10.1016/0034-4257(94)90136-8
Pezij, M., Augustijn, D. C. M., Hendriks, D. M. D., Weerts, A. H., Hummel, S., van der Velde, R., & Hulscher, S. J. M. H. (2019). State updating of root zone soil moisture estimates of an unsaturated zone metamodel for operational water resources management. *Journal of Hydrology X*, *4*(August), 100040. https://doi.org/10.1016/j.hydroa.2019.100040
Philip, S., Kew, S. F., van der Wiel, K., Wanders, N., & van Oldenborgh, G. J. (2020). Regional differentiation in climate change induced drought trends in the Netherlands. *Environmental Research Letters*. https://doi.org/10.1088/1748-9326/ab97ca
Potop, V., Turkott, L., & Koznarova, V. (2009). Drought Impact on Variability Crop Yields in Central Bohemia. *Cereal Research Communictaions*, *37*(2), 295–304. https://doi.org/10.1556/CRC.37.2009.2.18
Rahimi, Z. (2020). *Combined Sentinel-1 and - 2 soil moisture retrieval for a corn and wheat field in Twente*. University of Twente.
Roerink, G. J., Menenti, M., & Verhoef, W. (2000). Reconstructing cloudfree NDVI composites using Fourier analysis of time series. *International Journal of Remote Sensing*, *21*(9), 1911–1917. https://doi.org/10.1080/014311600209814
Roger, J. C., Vermote, E. . F., & Ray, J. P. (2011). *MODIS Surface Reflectance User ' s Guide*. 40.
Rouse, J. ., Haas, R. ., Schell, J. ., Deering, D. ., & Harlan, J. . (1974). *Monitroing the Vernal Adavancement and Retrogradation (Greenwave Effect) of Natural Vegetation* (Issue September 1972).
Sellers, P. J. (1987). Canopy reflectance, photosynthesis, and transpiration, II. The role of biophysics in the linearity of their interdependence. *Remote Sensing of Environment*, *21*(2), 143–183. https://doi.org/10.1016/0034-4257(87)90051-4
Sellers, P. J., Dickinson, R. E., Randall, D. A., Betts, A. K., Hall, F. G., Berry, J. A., Collatz, G. J., Denning, A. S., Mooney, H. A., Nobre, C. A., Sato, N., Field, C. B., & Henderson-Sellers, A. (1997). Modeling the exchanges of energy, water, and carbon between continents and the atmosphere. In *Science* (Vol. 275, Issue 5299, pp. 502–509). American Association for the Advancement of Science. https://doi.org/10.1126/science.275.5299.502
Seneviratne, S. I., Corti, T., Davin, E. L., Hirschi, M., Jaeger, E. B., Lehner, I., Orlowsky, B., & Teuling, A. J. (2010). Investigating soil moisture-climate interactions in a changing climate: A review. In *Earth-Science Reviews* (Vol. 99, Issues 3–4, pp. 125–161). Elsevier.

https://doi.org/10.1016/j.earscirev.2010.02.004
Sepulcre-Canto, G., Horion, S., Singleton, A., Carrao, H., & Vogt, J. (2012). Development of a Combined Drought Indicator to detect agricultural drought in Europe. *Natural Hazards and Earth System Science*, *12*(11), 3519–3531. https://doi.org/10.5194/nhess-12-3519-2012
Sims, A. P., Niyogi, D. D. S., & Raman, S. (2002). Adopting drought indices for estimating soil moisture: A North Carolina case study. *Geophysical Research Letters*, *29*(8), 2–5. https://doi.org/10.1029/2001GL013343
Sivakumar, V. K. M., Motha, P. R., Wilhite, A. D., & Wood, A. D. (2010). Quantification of Agricultural Drought for Effective Drought Mitigation and Preparedness: Key Issues and Challenges. *Agricultural Drought Indices Proceedings of a WMO Expert Meeting Held in Murcia, Spain*, *June*, 15.
Sluijter, R., Plieger, M., Oldenborgh, G. J. van, Beersma, J., & de Vries, H. (2018). Een analyse op basis van het potentiële neerslagtekort. *Knmi*. http://bibliotheek.knmi.nl/weerbrochures/droogterapport2018.pdf
Sobrino, J. A., Gómez, M., Jiménez-Muñoz, J. C., & Olioso, A. (2007). Application of a simple algorithm to estimate daily evapotranspiration from NOAA-AVHRR images for the Iberian Peninsula. *Remote Sensing of Environment*, *110*(2), 139–148. https://doi.org/10.1016/j.rse.2007.02.017
Spennemann, P. C., Rivera, J. A., Celeste Saulo, A., & Penalba, O. C. (2015). A comparison of GLDAS soil moisture anomalies against standardized precipitation index and multisatellite estimations over South America. *Journal of Hydrometeorology*, *16*(1), 158–171. https://doi.org/10.1175/JHM-D-13-0190.1
Spinoni, J., Naumann, G., Carrao, H., Barbosa, P., & Vogt, J. (2013). World drought frequency, duration, and severity for 1951-2010. *International Journal of Climatology*, *34*(8), 2792–2804. https://doi.org/10.1002/joc.3875
Stagge, J. H., Tallaksen, L. M., Xu, C. Y., & Van Lanen, H. A. J. (2014). Standardized precipitation-evapotranspiration index (SPEI): Sensitivity to potential evapotranspiration model and parameters. *IAHS-AISH Proceedings and Reports*, *363*(October), 367–373.
Svoboda, M., Lecomte, D., Hayes, M., Heim R, R., Gleason, K., Angel, J., Rippey, B., Tinker, R., Palecki, M., Stooksbury, D., Miskus, D., & Stephens, S. (2002). The Drought Monitor. *American Mete*, *April*.
Thenkabail, P. S., Gamage, M. S., & Smakhtin, V. U. (2004). *The Use of Remote Sensing Data for Drought Assessment and Monitoring in Southwest Asia*. http://www.iwmi.org
Tian, F., Fensholt, R., Verbesselt, J., Grogan, K., Horion, S., & Wang, Y. (2015). Evaluating temporal consistency of long-term global NDVI datasets for trend analysis. *Remote Sensing of Environment*, *163*, 326–340. https://doi.org/10.1016/j.rse.2015.03.031
Tirivarombo, S., Osupile, D., & Eliasson, P. (2018). Drought monitoring and analysis: Standardised Precipitation Evapotranspiration Index (SPEI) and Standardised Precipitation Index (SPI). *Physics and Chemistry of the Earth*, *106*, 1–10. https://doi.org/10.1016/j.pce.2018.07.001
Udelhoven, T., Stellmes, M., del Barrio, G., & Hill, J. (2009). Assessment of rainfall and NDVI anomalies in Spain (1989-1999) using distributed lag models. *International Journal of Remote Sensing*, *30*(8), 1961–1976. https://doi.org/10.1080/01431160802546829
USGS. (2020). *Statistical Methods in Water Resources Techniques and Methods 4 – A3*.
van den Hurk, B., Siegmund, P., Klein Tank, A., Attema, J., Bakker, A., Beersma, J., Bessembinder, J., Boers, R., Brandsma, T., van den Brink, H., Drijfhout, S., Eskes, H., & Haarsma, R. (2014). *KNMI'14: Climate Change scenarios for the 21st Century–A Netherlands perspective*. http://www.klimaatscenarios.nl/brochures/images/KNMI_WR_2014-01_version26May2014.pdf
Van Der Velde, R., Colliander, A., Pezij, M., Benninga, H.-J. F., Bindlish, R., Chan, S. K., Jackson, T. J., Hendriks, M. D., Augustijn, D. C. M., & Su, Z. (2021). Validation of SMAP L2 passive-only soil moisture products using upscaled in situ measurements collected in Twente, the Netherlands. *Hydrol. Earth Syst. Sci*, *25*, 473–495. https://doi.org/10.5194/hess-25-473-2021
van Hateren, T. C., Chini, M., Matgen, P., & Teuling, A. J. (2021). Ambiguous Agricultural Drought: Characterising Soil Moisture and Vegetation Droughts in Europe from Earth Observation. *Remote Sensing*, *13*(10), 1990. https://doi.org/10.3390/rs13101990
Van Loon, A. F. (2015). Hydrological drought explained. *WIREs Water*, *2*(4), 359–392. https://doi.org/10.1002/wat2.1085
Van Oijen, M., Balkovi, J., Beer, C., Cameron, D. R., Ciais, P., Cramer, W., Kato, T., Kuhnert, M., Martin, R., Myneni, R., Rammig, A., Rolinski, S., Soussana, J. F., Thonicke, K., Van Der Velde, M., & Xu, L. (2014). Impact of droughts on the carbon cycle in European vegetation: A probabilistic risk analysis using six vegetation models. *Biogeosciences*, *11*(22), 6357–6375. https://doi.org/10.5194/bg-11-6357-

2014
Vermote, F., Kotchenova, Y., & Ray, P. (2015). *MODIS Surface Reflectance User ' s Guide*. 40.
Vicente-Serrano, S., González-Hidalgo, J., de Luis, M., & Raventós, J. (2004). drought patterns in the Mediterranean area: the Valencia region (eastern Spain). *Climate Research*, *26*(1), 5–15. https://doi.org/10.3354/cr026005
Vicente-Serrano, S. M. (2007). Evaluating the impact of drought using remote sensing in a Mediterranean, Semi-arid Region. *Natural Hazards*, *40*(1), 173–208. https://doi.org/10.1007/s11069-006-0009-7
Vicente-Serrano, S. M., Beguería, S., & López-Moreno, J. I. (2011). Comment on Characteristics and trends in various forms of the Palmer Drought Severity Index (PDSI) during 1900-2008 by Aiguo Dai. *Journal of Geophysical Research Atmospheres*, *116*(19), 1–9. https://doi.org/10.1029/2011jd016410
Vicente-Serrano, S. M., Beguería, S., Lorenzo-Lacruz, J., Camarero, J. J., López-Moreno, J. I., Azorin-Molina, C., Revuelto, J., Morán-Tejeda, E., & Sanchez-Lorenzo, A. (2012). Performance of drought indices for ecological, agricultural, and hydrological applications. *Earth Interactions*, *16*(10). https://doi.org/10.1175/2012EI000434.1
Vicente-Serrano, S. M., Lo´pez, J. I., & Lo´pez-Moreno, L. (2010). A Multiscalar Drought Index Sensitive to Global Warming: The Standardized Precipitation Evapotranspiration Index. *Journals.Ametsoc.Org*, *23*(7), 1696–1718. https://doi.org/10.1175/2009JCLI2909.1
Vicente-Serrano, S. M., Beguería, S., & Lopez-Moreno, J. I. (2006). *A Multi-Scalar Drought Index Sensitive To Global Warming: the Standardized Precipitation Evapotranspiration Index – Spei*. 1–52.
Wang, L., Qu, J. J., Hao, X., & Zhu, Q. (2008). Sensitivity studies of the moisture effects on MODIS SWIR reflectance and vegetation water indices. *International Journal of Remote Sensing*, *29*(24), 7065–7075. https://doi.org/10.1080/01431160802226034
Weijers, R. (2020). *Drought indicators in The Netherlands*. *July*. https://repository.tudelft.nl/islandora/object/uuid:3c915a71-95ee-462d-99fc-eaa2fd167765
Werner, A. T., Prowse, T. D., & Bonsal, B. R. (2015). Characterizing the water balance of the Sooke Reservoir, British Columbia over the last century. *Climate*, *3*(1), 241–263. https://doi.org/10.3390/cli3010241
West, H., Quinn, N., Horswell, M., & White, P. (2018). Assessing vegetation response to soil moisture fluctuation under extreme drought using sentinel-2. *Water (Switzerland)*, *10*(7), 1–22. https://doi.org/10.3390/w10070838
Wgnn, J., & Vmi, C. (2020). *Investigate the Sensitivity of the Satellite-Based Agricultural Drought Indices to Monitor the Drought Condition of Paddy and Introduction to Enhanced Multi-Temporal Drought Indices*. https://doi.org/10.35248/2469-4134.20.9.272
Wit, A. De, & Su, B. (2005). Deriving phenological indicators from SPOT-VGT data using the HANTS algorithm. *2nd International SPOT-VEGETATION User Conference*, *1*, 195–201. ftp://ftp.ccrs.nrcan.gc.ca/ad/Phenology/PhenologyPapers/Dewit_2004_SPOTVGT_Phenology_Netherlands.pdf
Wu, H., Svoboda, M. D., Hayes, M. J., Wilhite, D. A., & Wen, F. (2007). Appropriate application of the Standardized Precipitation Index in arid locations and dry seasons. *International Journal of Climatology*, *27*(1), 65–79. https://doi.org/10.1002/joc.1371
Yihdego, Y., Vaheddoost, B., & Al-Weshah, R. A. (2019). Drought indices and indicators revisited. *Arabian Journal of Geosciences*, *12*(3). https://doi.org/10.1007/s12517-019-4237-z
Zargar, A., Sadiq, R., Naser, B., & Khan, F. I. (2011). A review of drought indices. *Environmental Reviews*, *19*, 333–349. https://doi.org/10.1139/A11-013
Zhang, M., & Yuan, X. (2020). Rapid reduction in ecosystem productivity caused by flash droughts based on decade-long FLUXNET observations. *Hydrol. Earth Syst. Sci*, *24*, 5579–5593. https://doi.org/10.5194/hess-24-5579-2020